General Disclaimer

One or more of the Following Statements may affect this Document

- This document has been reproduced from the best copy furnished by the organizational source. It is being released in the interest of making available as much information as possible.

- This document may contain data, which exceeds the sheet parameters. It was furnished in this condition by the organizational source and is the best copy available.

- This document may contain tone-on-tone or color graphs, charts and/or pictures, which have been reproduced in black and white.

- This document is paginated as submitted by the original source.

- Portions of this document are not fully legible due to the historical nature of some of the material. However, it is the best reproduction available from the original submission.

Produced by the NASA Center for Aerospace Information (CASI)

SOLID STATE IMAGE SENSOR RESEARCH

W. H. HELL, A. R. ASAM, R. W. HAAS

JULY 1968

CONTRACT NO. NAS 12-553

Prepared By

THE MARQUARDT CORPORATION

16555 Saticoy Street
Van Nuys, California

For

NATIONAL AERONAUTICS AND SPACE ADMINISTATION

ELECTRONICS RESEARCH CENTER

CAMBRIDGE, MASSACHUSETTS

SOLID STATE IMAGE SENSOR RESEARCH

By W. Hell, A. Asam, and R. Haas

July 1968

TABLE OF CONTENTS

LIST OF ILLUSTRATIONS

LIST OF ILLUSTRATIONS (continued)

By W. Hell, A. Asam, and R. Haas

The Marquardt Corporation
Van Nuys, California

SUMMARY

The objective of this contract was to adapt Marquardt's sensing
techniques to image sensing devices for meteorological satellite and re-
lated applications and investigate its performance capabilities relative
to these applications in the visible spectrum. A tradeoff design study
indicated theoretically that an illumination range of 120:1 and a matrix
of 3,000 x 3,000 image points could be achieved with the present materials.
A unique ferroelectric material process for the thin film deposition of
lead titanate zirconate was developed but further work is necessary to
produce uniform areas of 1 x 1 inches. Several image plates were fabri-
cated but due to the limitations in the ferroelectric material, a reason-
able performance was not obtained from any large capacity plate. Functions
of sensing, storage, and readout were demonstrated with a six element line
array.

INTRODUCTION

This report describes the work performed in the Contract NAS 12-553 for the period May 1967 through 30 June 1968. The primary objective was to adapt the Marquardt Ferrotron sensing technique to image transducer devices suited for meteorological satellite application. The immediate goal was to establish a method for the preparation of an image plate which is the nucleus of such a device and to evaluate its performance characteristics by means of a limited breadboard.

A main concern in space image sensors is (1) the large dynamic tone range required when exposing simultaneously a partial night/partial day illuminated scene and (2) the image retention capability required when exposure time and frame readout time are not analogous. The Ferrotron image transducer concept would fulfill these requirements. It is based on a thin film laminate of photoconductor material for the image sensing function and a ferroelectric material for retaining the latent image. During exposure the incident photons from a scene control the current flowing through the photoconductor at each point of the image. The ferroelectric material, in turn, integrates these currents by internal polarization and permanently stores a charge pattern of the image until readout. Commutators integrated with this image plate by thin film techniques scan the latent image during readout at a rate compatible with the bandwidths of the transmission link to produce video signals.

The dual material approach allows an image transducer implementation that would inherently feature, once developed, high sensitivity, large tone scale, fine resolution and a high signal-to-noise ratio besides the advantages realized in space applications by the solid state approach, such as low power requirements, small size and weight, extreme reliability and long life.

Under previous efforts, the feasibility of the Ferrotron concept and the validity of its features has been proven experimentally by means of discrete sensor elements. Furthermore, the development of economical techniques for the preparation of larger area sensing plates had been in progress. For example, a process technique for the deposition of large area thin film photoconductors was nearly developed. These photoconductors can be operated in the volume mode where the current flows through the layer rather than along its surface as commonly operated. The capability of operating in the volume mode is essential for producing high resolution image plates. This photoconductor exhibits a very large dynamic range of 9 orders of magnitude and a low light level response of 10^{-6} footcandles. Although these films had been deposited over areas as large as 3 x 3 inches, improvements of the process techniques were required to eliminate pinholes which would render the film useless in

2

this application. To date, a satisfactory photoconductor material is available where the process technique is well enough defined to allow the optimization of its performance characteristics for specific applications.

A ferroelectric material has been previously produced, by epitaxial growth and subsequent cleaving and polishing, that exhibits satisfactory performance characteristics. However, its low Curie temperature would not allow the deposition of the photoconductor, requiring a temperature of $600^{\circ}C$ for post activation, for the formation of an image plate laminate. In this program then a ceramic ferroelectric was obtained as an alternate that could withstand this temperature. With this material it was successfully demonstrated that a photoconductor can be deposited onto a ferroelectric and it was proven that physical and chemical compatibility exists between the two materials, i.e., no deterioration in performance characteristic was observed with repeated operation. However, it was found that the ferroelectric material could not be produced thin enough to reduce its coercive voltage to a value safely below the breakdown voltage of a volume photoconductor. In further image plate experimentation, therefore, the photoconductor was operated in a combination surface/volume mode which is less desirable because it reduces the plate's resolution capability. Nevertheless, these experiments demonstrated successfully that the Ferrotron mechanism can be applied to area type device configuration.

In order to read out the latent image stored in the ferroelectric, it is necessary to increase the conductivity of the photoconductor element by element beyond its normal operating value. An elemental high conductivity can be obtained either by a high intensity light beam sweeping over the plate or by driving the photoconductor into space charge condition with a high voltage applied to each element via a commutated electrode matrix. Although the latter method is more desirable in the contemplated space image transducer, the light beam method had to be used in the above experiments because of the ferroelectric/photoconductor voltage incompatibility.

It was then decided to initiate, in conjunction with another program, the development of a thin film process for the preparation of this ferroelectric material that would overcome the voltage limitation. To date, the specific process for the preparation of a satisfactory thin film material has been established which in itself is a state-of-the-art advancement; however, the application of this new technology to the fabrication of a large area image plate requires an additional effort.

REQUIREMENTS

The performance characteristics of an image sensor are generally defined by parameters pertaining to (1) image quality and (2) data flow rate. Image quality depends on the resolution with which geometric scene details can be discriminated or the total number of elements into which the image can be dissected for transmission signals. In a meteorological satellite application for the visible region, a relatively coarse TV-like resolution of 500 x 500 elements is acceptable when only little information detail is contained in a scene. A finer resolution, e.g., 2000 x 2000 elements, is required when the scene contents are approaching photographic detail. Another parameter characterizing image quality depends on the tone scale or contrast capability with which light intensity levels can be discriminated. Typically, a low quality picture requires a tone scale of one order of magnitude discriminating 8 possible shades of gray and a high quality picture two to three orders of magnitude with 21 shades of gray. The number of discernable tone levels determines the minimum required signal-to-noise ratio which in the latter case is 60 db.

The operating range of the image transducer is determined by the scene illumination which is as high as 10^4 footcandles by day and as low as 10^{-5} footcandles by night. This large difference is desirable where resistivity and exposure time can be varied over a wide range. A special condition exists when the scene is partially in the dark and partially in the light.

The data flow rate in an image transducer depends on the image frame frequency and the number of dissected image elements. The frame frequency in a meteorological satellite application is dictated by the speed of the satellite over ground and the field of view covered by each frame. Typically, the apparent ground speed is 3.3 miles per second when orbiting at 600 miles altitude and the ground coverage is 1000 miles per frame at a resolution of 1 mile. Assuming a scene continuum the slowest permissible frame frequency is 300 seconds.

Unless the optics of the image sensor are caused to remain fixed in the direction of a scene under consideration, the relative satellite motion will cause a deterioration in image resolution. Restricting such a deterioration to an acceptable 10% of a resolution element or .1 mile, the total frame sensing time is limited to 0.03 seconds. The large difference between allowable sensing time and minimum frame frequency indicates that a photo camera mode of operation is desirable where the latent image of a scene is stored with a relatively short exposure time and where this image is read out for transmission during the remainder of the frame time. Separating the exposure and the readout functions results in the contemplated application, a slow data flow rate that can be transmitted via a narrow bandwidth transmission exhibiting a signal-to-noise advantage.

4

FERROTRON IMAGE TRANSDUCER CONCEPT

The concept of Marquardt's thin film solid state sensor/scanner plate or image transducer capable of satisfying many advanced image sensing functions is described below. The general image transducer plate configuration is shown in Figure 1. It is a single laminate of solid state materials for performing the two functions of image transducing, i.e., the sensing/storage and the readout/ commutating functions. Fine electrode lines are deposited on each side of the laminate orthogonally to each other, thereby dividing the sensor plate effectively into small elemental areas for readout purposes. Either a continuous exposure mode or a frame exposure mode of operation could be employed. In the latter case, an electric shutter pulse exposes effectively the sensing area to the projected image. The optical image is thereby transduced into a latent image in the form of a charge pattern which is retained until readout. The stored image is read out by rapidly commutating the rows and columns of the electrode matrix. Each switched matrix point produces a video signal proportional to the stored charge.

The sensing portion of the image transducer plate is composed of thin film layers of photoconductor/ferroelectric/electrode materials and a supporting glass substrate. The front electrode is transparent to allow the light from the scene to reach the photoconductor. An elemental area of the laminate and an equivalent circuit is shown in Figure 2. The photo- conductor (PC) can be thought of as a variable resistor whose conductivity is approximately proportional to the intensity of the incident light (Figure 3). The ferroelectric (FE) can be thought of as a non-linear capacitor across which an internal polarization (charge) is accumulated as a function of the time integral of the current flow. The internal polarization of the FE follows a voltage/charge hysteresis pattern analogous to the more familiar ferromagnetic B/H hysteresis phenomena. The stored charge, i.e., internal polarization, will not leak off in time as occurs with the charge in purely dielectric materials employed in conventional capacitors. As a result, there is no loss in the analog signal amplitude between exposure and readin oper- ations.

In operation, light impinging on an element from a radiant source will cause the photoconductor to become more conductive than in its dark state. During exposure, a voltage is applied across the element causing current, determined by the PC resistance, to flow through the photoconductor and charge up the FE material. The charge value is retained until an opposite voltage is applied for readout. Since a fractional polarization is a function of photoconductor current and time duration of the readin pulse applied to it, it represents a grey scale of an image point (Figure 4). The dynamic range and thereby the gamma of the sensor can be varied by changing the
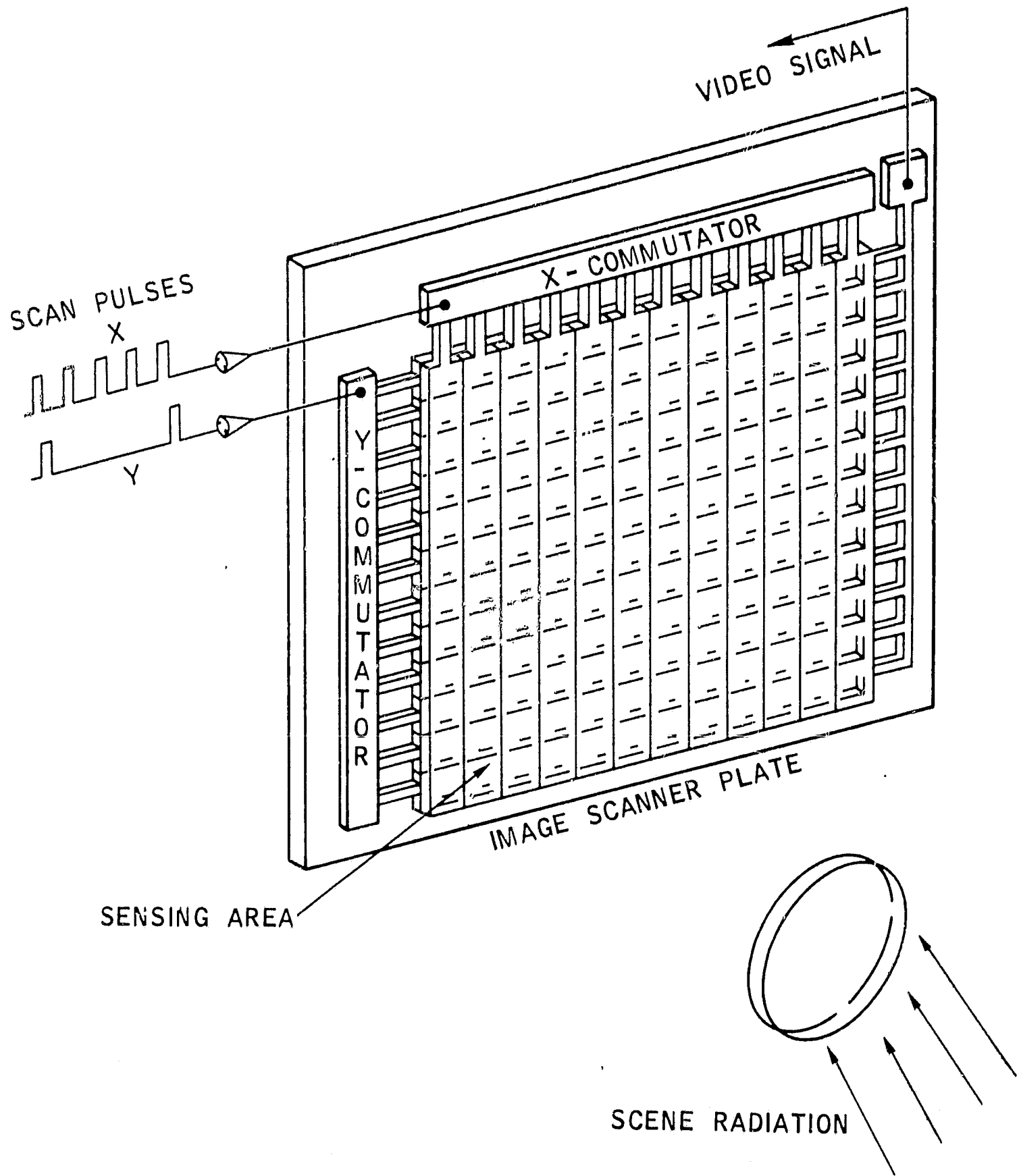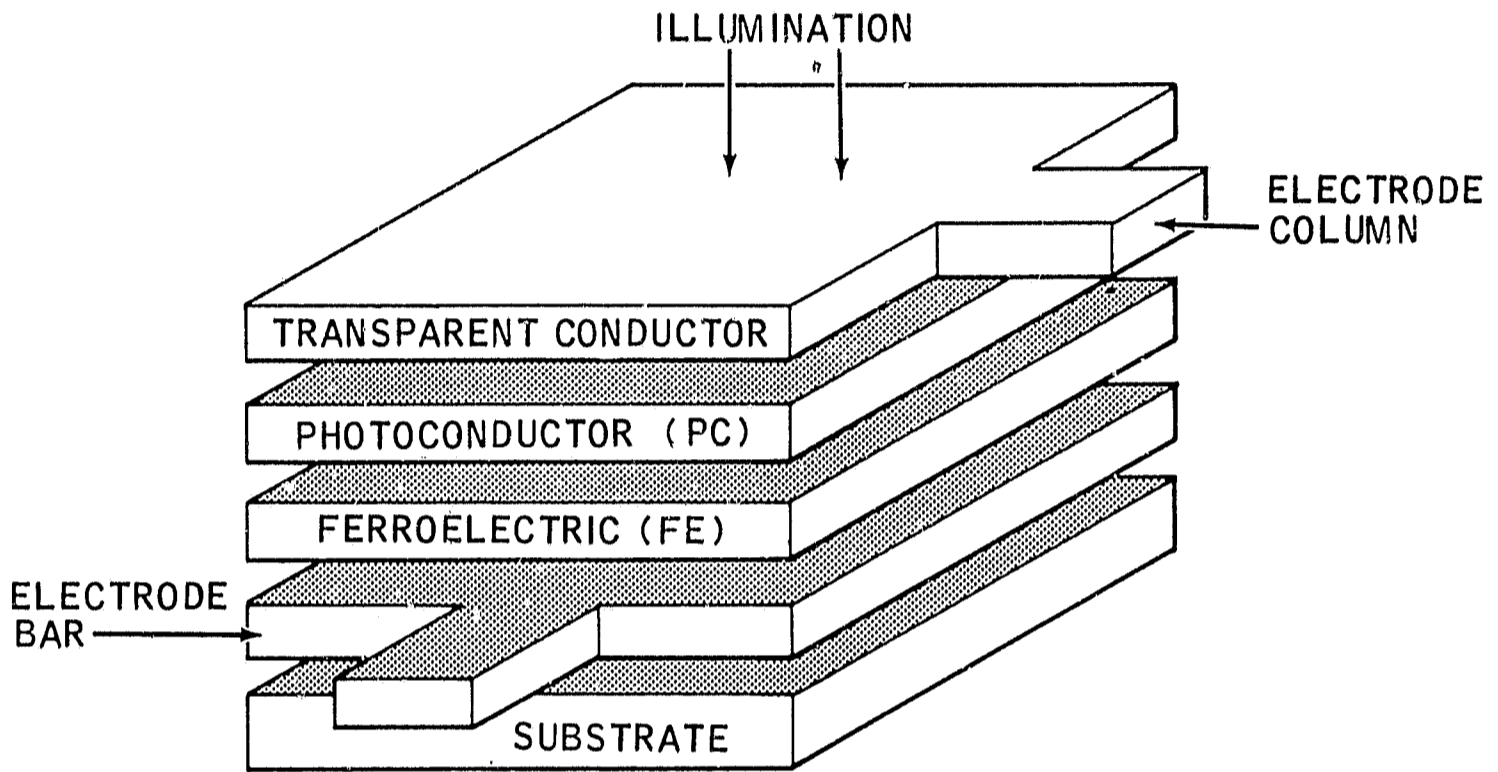
Figure 1

IMAGE SENSOR WITH OPTO-ELECTRONIC READ OUT

ILLUMINATION

TRANSPARENT CONDUCTOR

PHOTOCONDUCTOR (PC)

FERROELECTRIC (FE)

ELECTRODE
COLUMN

ELECTRODE
BAR

SUBSTRATE

A. LAMINATE

READ   EXPOSE   ILLUMINATION

PC

B−   B+   FE
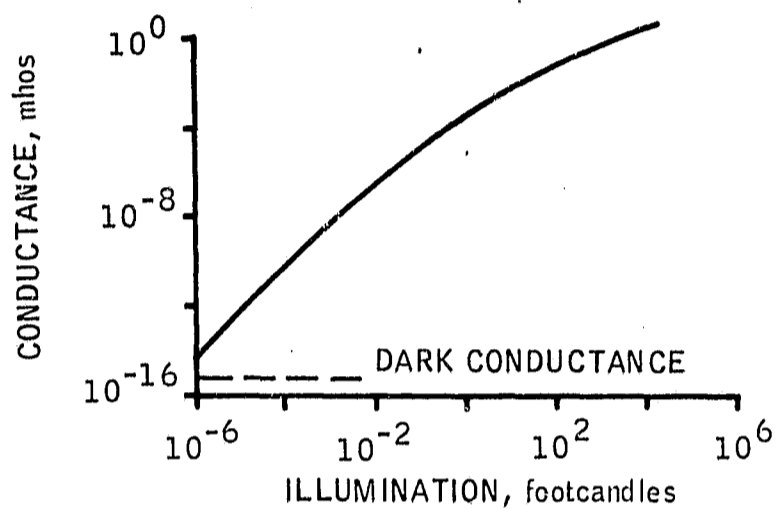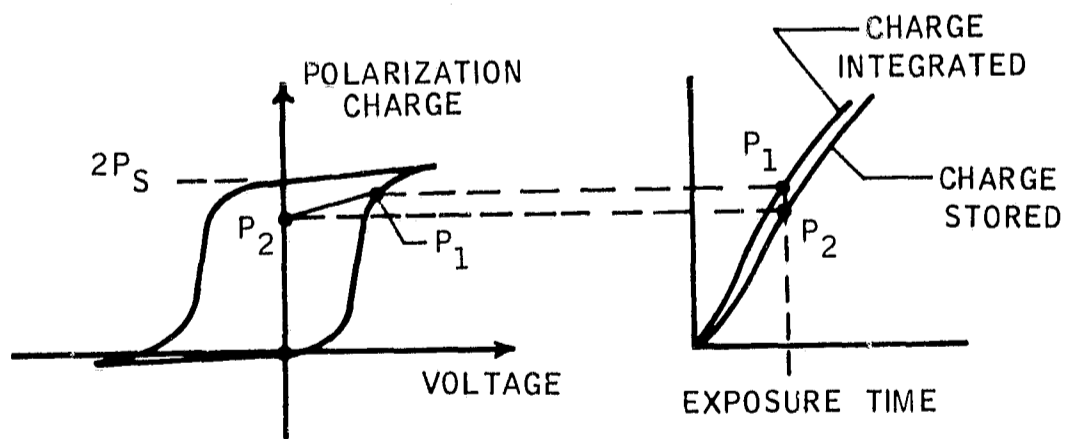
OUTPUT
SIGNAL
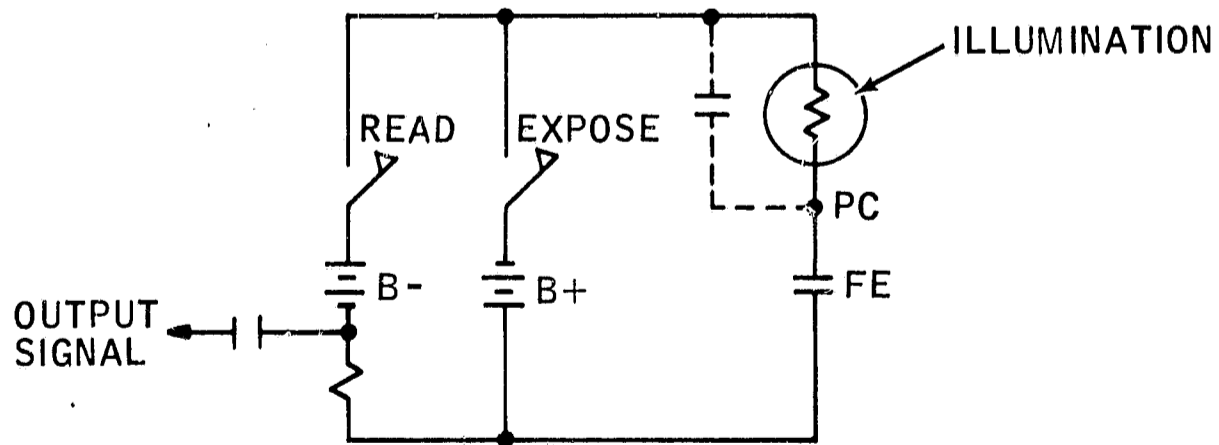
B. EQUIVALENT CIRCUIT

Figure 2

SENSOR ELEMENT

R−22,603

(A) CdS PHOTO CONDUCTOR

(B) CHARGE RETENTION BY A NON-LINEAR FERROELECTRIC CAPACITOR

Figure 3

IMAGE PLATE MATERIAL CHARACTERISTICS

STORAGE   MEDIA   LIGHT   SENSITIVE
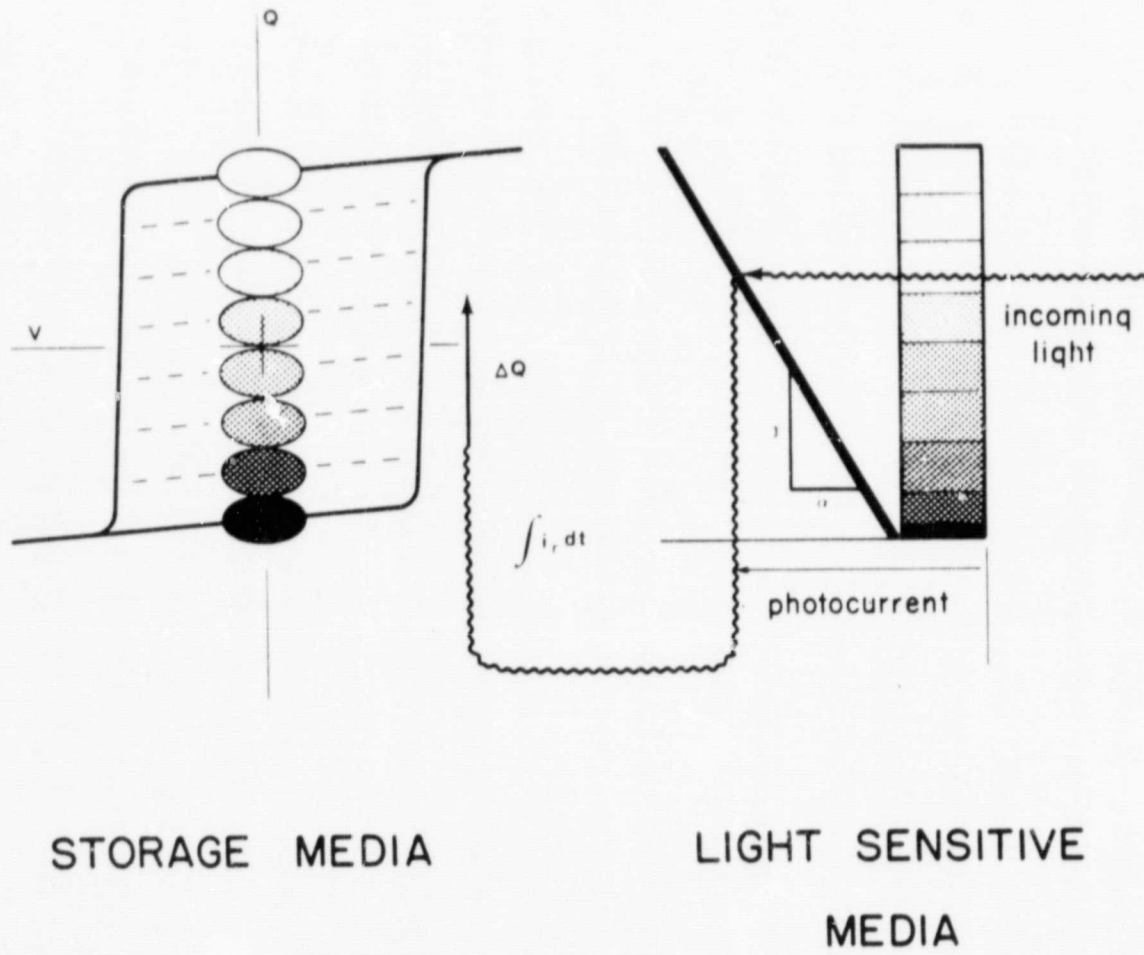   MEDIA

Figure 4

RELATION OF GRAY SCALE TO POLARIZATION

amplitude and time duration of the readin voltage applied to it. The application of an opposite voltage to the ferroelectric element results in a current which discharges the stored data and returns the FE material to its original state of polarization. To effect the ferroelectric readout it is necessary to lower the resistance of the photoconductor. For this purpose, the photoconductor is driven into its space charge limited state by the application of a high electric field which will result in the delivery of a very high current to the FE independent of illumination (Figure 5).

Figure 6 shows a complete write/read cycle where the readout current time integral is proportional to the readin current time integral, which, in turn, is representative of the light intensity at that image point. Inasmuch as the readout time is considerably shorter than the exposure time, a high current level, low impedance output signal is realized.

In the image sensor plate an elemental readout current is obtained at the intersection point of the front electrode bar and back electrode column pair that is switched on. The desired sequence of bar and column switching would depend on the particular application requirements. For example, in a conventional image transducer application a raster mode scan sequence would be employed. In this case, the electrode bars are switched on in incremental steps. At each "bar" step position, all the columns are switched one after another in rapid sequence. In this manner, the latent image is dissected point by point producing the appropriate video signals required to transduce a complete image.
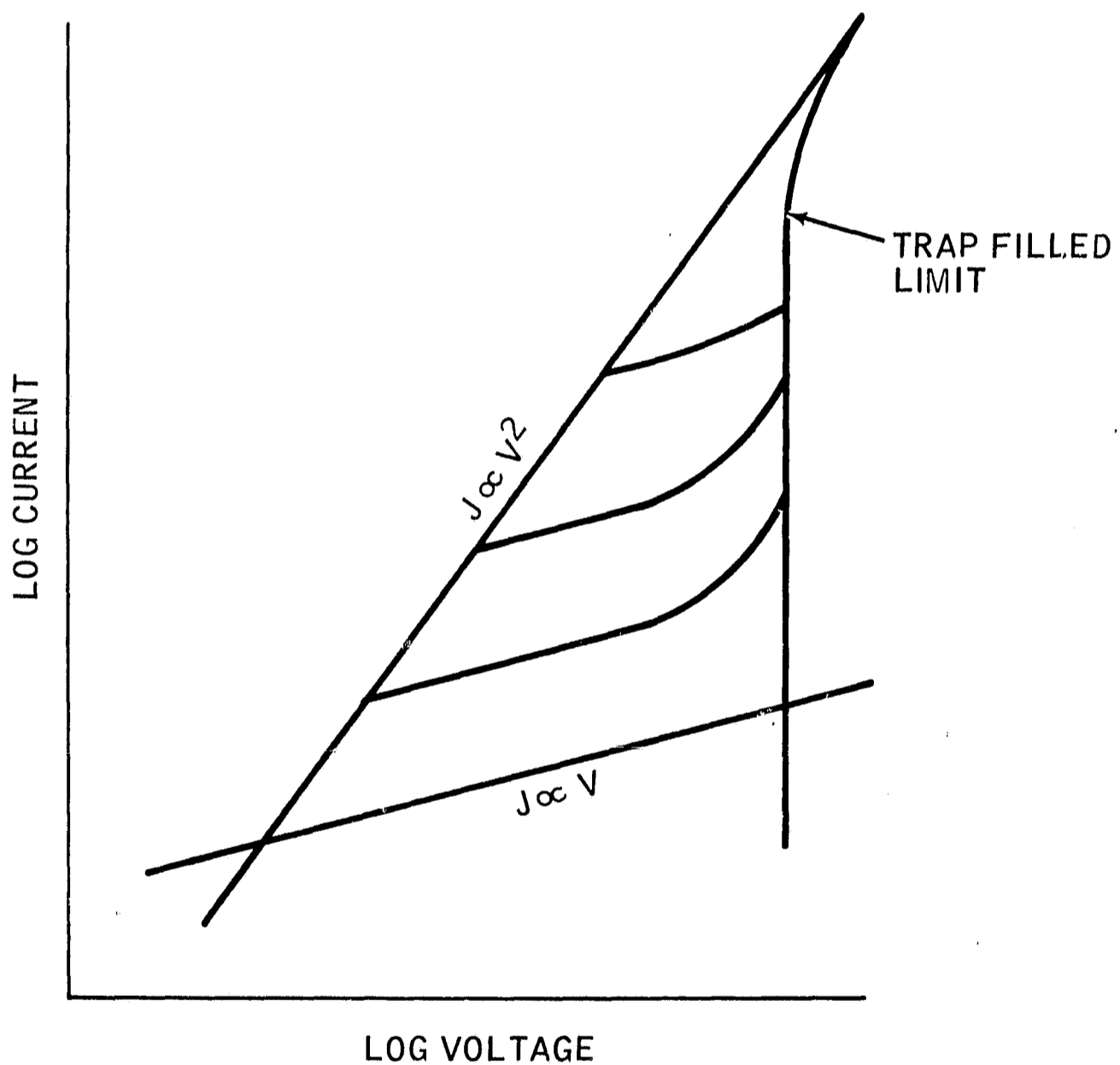
AS INDICATED BY THE TRAP FILLED LIMIT LINE, THE CURRENT
(AND HENCE CONDUCTIVITY) OF A PHOTOCONDUCTOR
BECOMES VERY LARGE AND INDEPENDENT OF ILLUMINATION
FOR SUFFICIENTLY LARGE APPLIED VOLTAGE.

Figure 5

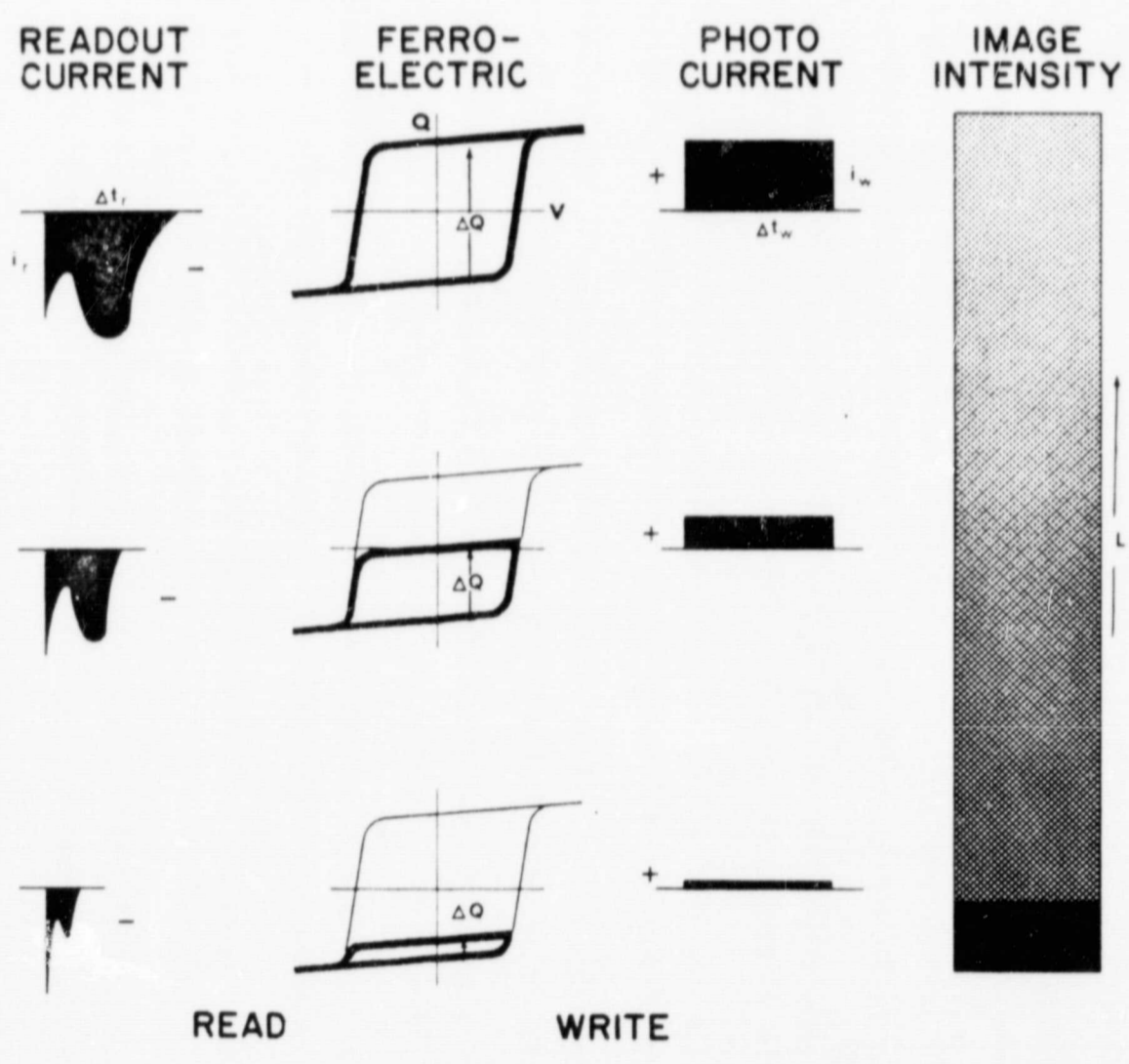SPACE CHARGE LIMITATION OF A TYPICAL PHOTOCONDUCTOR

Figure 6

WRITE / READ CYCLE

IMAGE PLATE DESIGN CONSIDERATIONS

As previously described, the image plate consists of a laminate of ferroelectric and photoconductor material. The function of the photoconductor is to provide a resistive circuit component which is proportional to the incident illumination. This high impedance determines the flow of current in the circuit. The function of the ferroelectric is to integrate this current over a fixed interval of time and store the resultant charge for later readout. It is necessary to select both the photoconductor and ferroelectric materials to satisfy this basic energy compatibility. In addition, other system considerations such as the total number of image points, the total time of exposure and readout, the dynamic range or illumination contrast, and the gain together with the limitations of the materials themselves must guide the selection.

The charge that can be stored in the ferroelectric by virtue of the hysteresis loop is proportional to the spontaneous polarization and the size of the element area.

$$Q_{FE} = 2 A P s$$

where A = area in cm^2

Ps = polarization in coulombs cm^{-2}

The charge provided by the photoconductor is proportional to the photoconductor current and the time of current flow during exposure time, t_w

$$Q_{pc} = i_{pc} t_w$$

The steady state current that is furnished by the photoconductor during exposure is

$$i_{pc} = K L^\alpha V^\beta$$

where K = constant related to geometry of cell and specific
L = intensity of illumination   material
V = applied voltage

α = coefficient representing overall quantum efficiency of cell. This coefficient can be determined from the slope of a photocurrent versus illumination curve

β = voltage coefficient related to processing methods. This coefficient can be determined from the slope of a photocurrent versus voltage curve.

For example, α values include such factors as the effect of different donor and acceptor levels introduced into the crystal during the material processing, the degree of doping, reflective coefficients of the surface, etc. From these measurements, then, the process can be modified to compensate for deficiencies in the doping constituents. The voltage exponent, β, describes the current-voltage relationship and depends, besides other factors, on the ratio of work functions between the host crystal, CdS, and the electrode materials. (See Figures 7 and 8.)

Figure 9 describes the hysteresis loop for a typical ferroelectric element. As can be seen, Q_M represents the maximum charge that can be stored in an element with a given area and Q_m represents the minimum charge. The ratio of these charges provides a rough measure of the squareness of the hysteresis loop, S.

$$S \cong \frac{Q_M}{Q_m}$$

Since the photoconductor must deliver the charge in each case,

$$Q_M = K L_1^{\alpha} V^{\beta} t_w$$

$$\text{and} \quad Q_m = K L_2^{\alpha} V^{\beta} t_w$$

substituting,

$$S = \frac{Q_M}{Q_m} = \frac{K L_1^{\alpha} V^{\beta} t_w}{K L_2^{\alpha} V^{\beta} t_w}$$

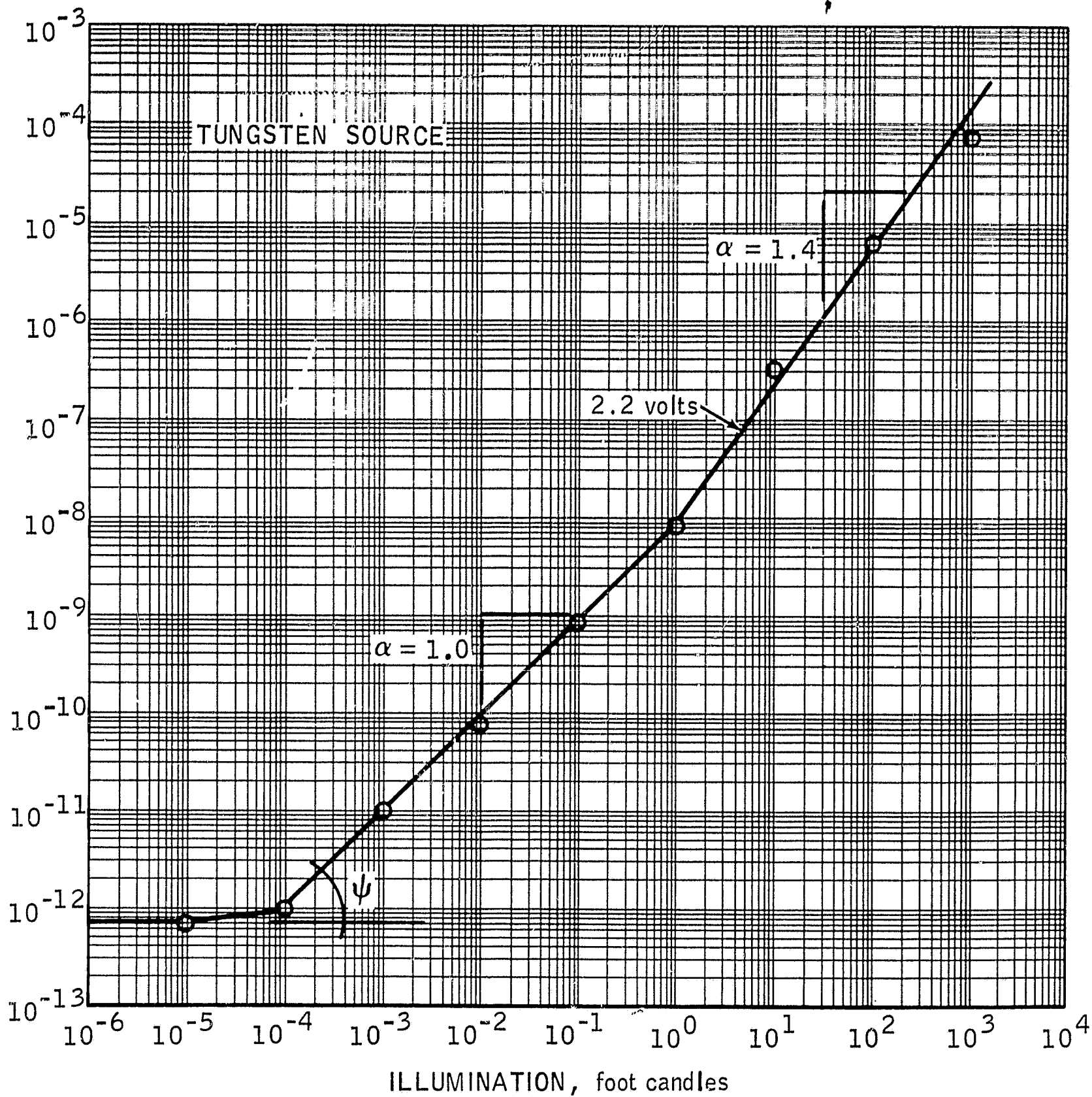$$S^{\frac{1}{\alpha}} = \frac{L_2}{L_1}$$

Figure 7
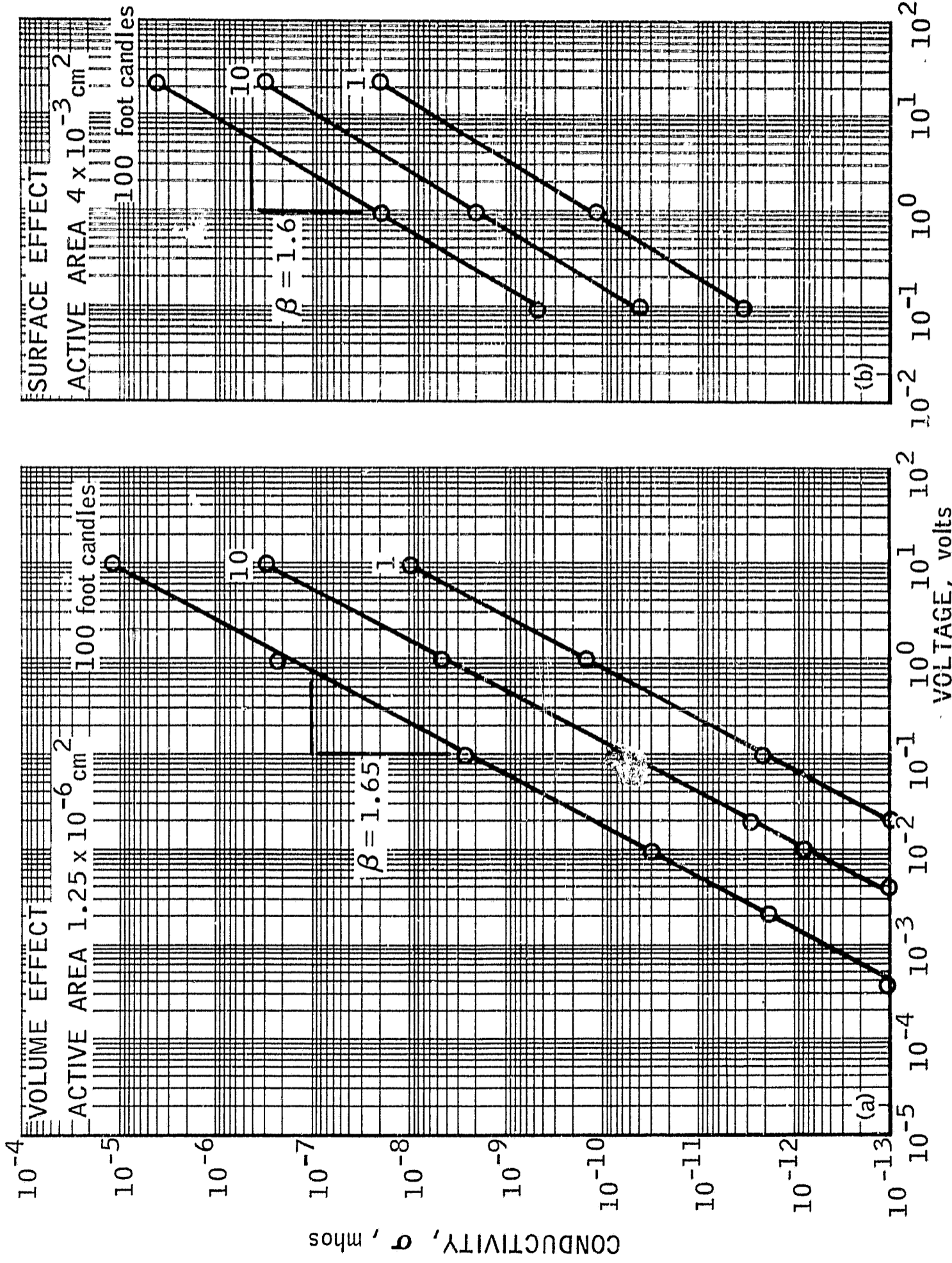
CONDUCTIVITY AS A FUNCTION OF ILLUMINATION
(RUN NO. 9.06)

PHOTOCONDUCTOR CONDUCTIVITY vs. VOLTAGE
Figure 8
(RUN NO. 9.05)

SATURATION HYSTERESIS LOOP
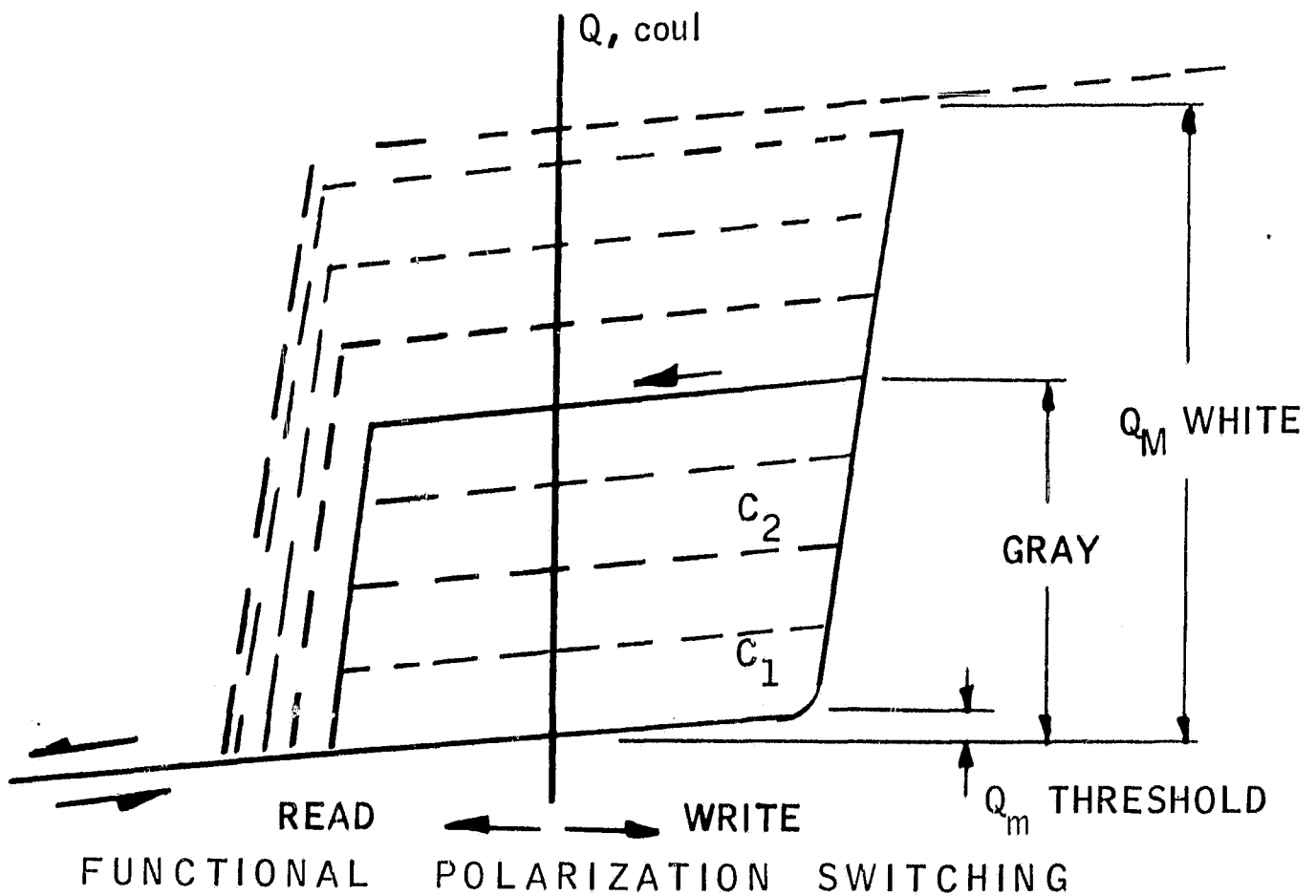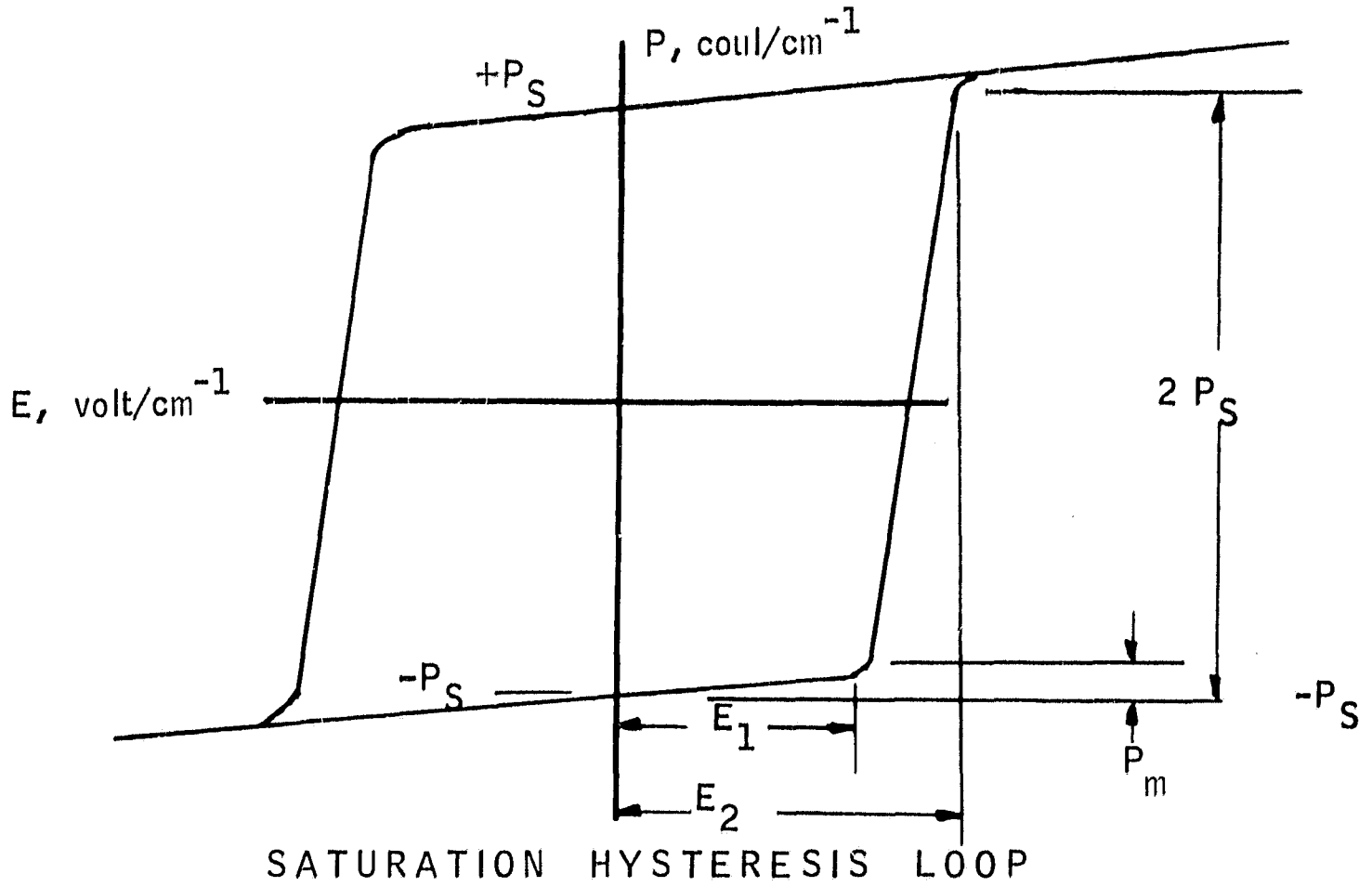
FUNCTIONAL POLARIZATION SWITCHING

Figure 9

HYSTERESIS LOOPS

The coefficient, α, can be varied in the Marquardt photoconductor by slight modifications of the processing. Factors of S equal to 120 have easily been achieved in the thin film ferroelectric. For a representative value of $\alpha = 1$,

$$120\ L_1 = L_2$$

therefore,

$$L_1 = 1 \text{ footcandle} \qquad L_2 = 120 \text{ footcandles}$$

$$L_1 = 8 \text{ foot candles} \qquad L_2 = 1000 \text{ footcandles}$$

In an image plate featuring storage capability, one criteria for determining the total number of image points is the degradation of stored image data suffered during the readout cycle. As discussed previously, readout in an optical scan mode is accomplished by the application of voltage and sequential incident illumination on each image elemental area. As the plate is scanned, a dark current will flow in the unscanned elements. The time that current will flow in the last element to be scanned is approximately equal to the total scan time. Since the flow of this current with time represents delivered charge, a degradation of stored charge available for readout will occur.

The dark resistance, $R_D = \rho \dfrac{\ell}{BW}$

where ρ = resistivity in ohm cm^{-1}

ℓ = material thickness, cm

$B = W$ = element dimension in cm

The dark current per element, $I_D = \dfrac{V}{R_D}$

The loss in charge

$$Q_D = (n - 1) \dfrac{V}{R_D}\ t_r$$

where n = total number of elements

t_r = readout time per element

Since the total charge that can be stored per image point is

$$Q_{FE} = 2\ APs = 2\ BWPs$$

The percentage of degradation from this contribution is

$$D = \frac{Q_D}{Q_{FE}} = \frac{(n-1) \frac{V}{R_D} t_r}{2\ BWPs}$$

$$= \frac{(n-1)\ V\ BW\ t_r}{2\ BWPs\ \rho_D\ \ell} = \frac{(n-1)\ V\ t_r}{2\ Ps\ \rho_D\ \ell}$$

The time of readout for an elemental area is related to the light resistance that can be achieved with a given photoconductor material.

$$\text{Since}\quad t_r = \frac{Q_M}{i_{pc}}$$

$$= \frac{Q_M}{V} R_L = \frac{Q_M}{V} \frac{\rho_L \ell}{BW} = \frac{2\ BWPs}{V} \frac{\rho_L \ell}{BW}$$

Substituting in the above equation, $\qquad = \dfrac{2\ Ps\ \rho_L\ \ell}{V}$

$$D = \frac{(n-1)\ V\ t_r}{2\ Ps\ \rho_D\ \ell} = \frac{(n-1)\ V}{2\ Ps\ \rho_D\ \ell} = \frac{2\ Ps\ \rho_L\ \ell}{V}$$

$$= \frac{(n-1)\ \rho_L}{\rho_D}$$

Ratios of dark to light resistivities of 10^9 can be reliably achieved with the Marquardt thin film photoconductor. Therefore, the ratio $\dfrac{\rho_L}{\rho_D}$ would equal 10^{-9} in the formulation.

the equation becomes,

$$D = (n-1)\ 10^{-9} \text{ and,}$$

if a degradation of 1% is assumed,

$$n-1 = \frac{10^{-2}}{10^{-9}} = 10^{7}$$

and a matrix of 3,000 x 3,000 could be achieved.

The gain, maximum resolution, and capacity that can be achieved in a meteorological image sensor is also a function of the geometry of the individual sensing elements. To make such a determination both the surface and volume configurations of the photoconductor should be considered (See Figure 10). The gain or apparent quantum efficiency in each case is

Surface Mode

$$G = \frac{\tau}{T_{T}} = \frac{\tau \mu V}{W^{2}}$$

Volume Mode

$$G = \frac{\tau}{T_{T}} = \frac{\tau \mu V}{d^{2}}$$

where τ = lifetime in seconds

T_{T} = transit time in seconds

μ = mobility in cm^{2} $volt^{-1}$ sec^{-1}

W = gap width in surface case in cm

d = gap width in volume case in cm

V = operating voltage

The current drawn from any element is

$$I = eFG$$

where e = electron charge in coulombs

F = rate of electrons generated in seconds

The assumption will be made that the surface dimensions are equal and, therefore, equal surface areas exist for each configuration.

From the above it can be seen that the gain in the volume mode is greater by a factor of $\frac{W^{2}}{d^{2}}$ than that of the surface mode. By conventional
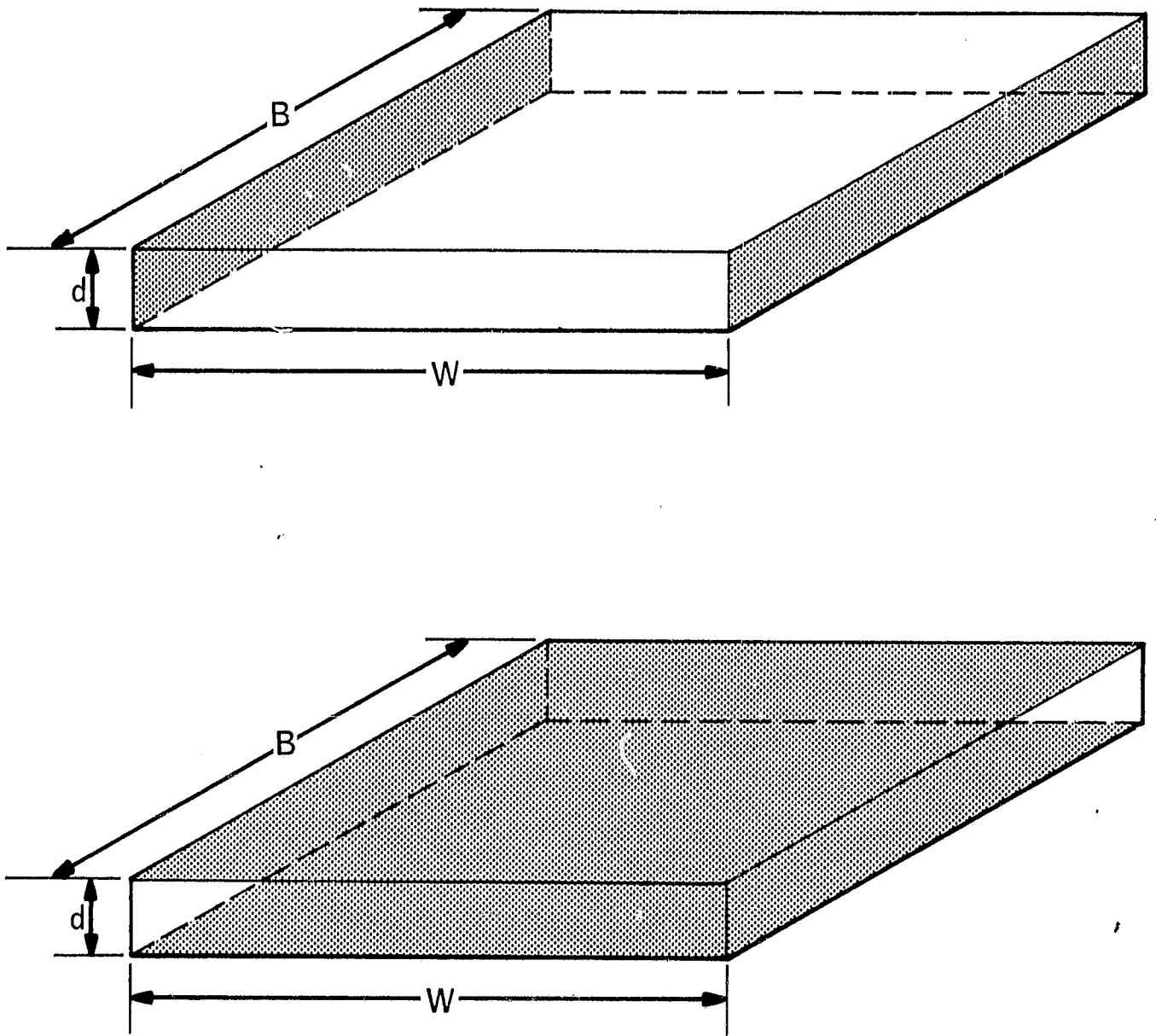
20

Figure 10

PHOTOCONDUCTOR CONFIGURATIONS

masking techniques, W will be a minimum of approximately 1 mil. The thickness of the thin film photoconductors produced at TMC is approximately 2 microns. The difference in gain is $\dfrac{(40)^2}{(2)^2} = \dfrac{1600}{4} = 400.$

As discussed above, resistance becomes an important parameter in determining the number of total points in an image plate.

The light resistance and dark resistance for the two cases

Surface

$$R_{LS} = \rho \, \frac{W}{Bd}$$

Volume

$$R_{LV} = \rho \, \frac{d}{WB}$$

$$\frac{R_{LS}}{R_{LV}} = \frac{\rho W}{Bd} \cdot \frac{WB}{\rho d} = \frac{W^2}{d^2}$$

Using the above dimensions, it can be seen that R_D and R_L in the surface mode is 400 times greater than the volume mode. However, the ratio for each configuration remains the same and the limit of the total number of points would be the same.

IMAGE PLATE DEVELOPMENT

Experimentation

Two image plate configurations were fabricated using the previously mentioned ceramic ferroelectric of lead titanate zirconate. The ferroelectric material was lapped and polished to a thickness of approximately one mil. A thinner layer could not be obtained because of mechanical handling problems. The thickness of the thin film photoconductive layer (3 microns) for the sensor plate was optimumly selected on the basis of the absorption coefficient of the material and the diffusion length of a carrier. A design paradox existed since the operating voltage division between the layers required a voltage sufficient to switch the ferroelectric into saturation and a voltage low enough to avoid breakdown in the photoconductor. For an image plate with a volume configuration, most of the voltage will appear across a dark photoconductor due to the high dark resistance. When light is applied, however, sufficient voltage appears across the ferroelectric to cause switching.

Since the dielectric breakdown field of this type of photoconductor is approximately 10^5 volts cm^{-1}, the voltage necessary to switch a one mil ferroelectric approaches this limitation. Therefore, two configurations were designed and fabricated in an attempt to provide an operable device.

The first sensor plate contained approximately 100 x 100 3 mil elements on 4 mil centers (See Figure 11). The plate was designed to operate in the volume mode. The thickness of the photoconductive layer was approximately 40 microns which was sufficient to overcome the breakdown condition but provided a more inefficient photoconductor with greater losses. The ferroelectric layer was electroded on the bottom with a solid gold electrode and on the top with the above elemental electrodes. The common electrode was silver soldered to a stainless steel substrate. The photoconductor was then deposited on this combination. A conducting glass served as the top transparent electrode. Subsequent testing of this plate indicated that only a few points were operable. When the whole plate was flooded with illumination and cycled, the composite hysteresis loop showed that the losses of the photoconductor combined with the ceramic ferroelectric were too great for adequate isolation during readout. Consequently, this approach was temporarily abandoned.

A hybrid configuration that can use the wider gap of the surface mode photoconductor but operates in the volume mode was selected as a compromise. A one mil layer of ferroelectric was gold electroded with a bar pattern on the bottom side and a dot pattern on the top. A thin
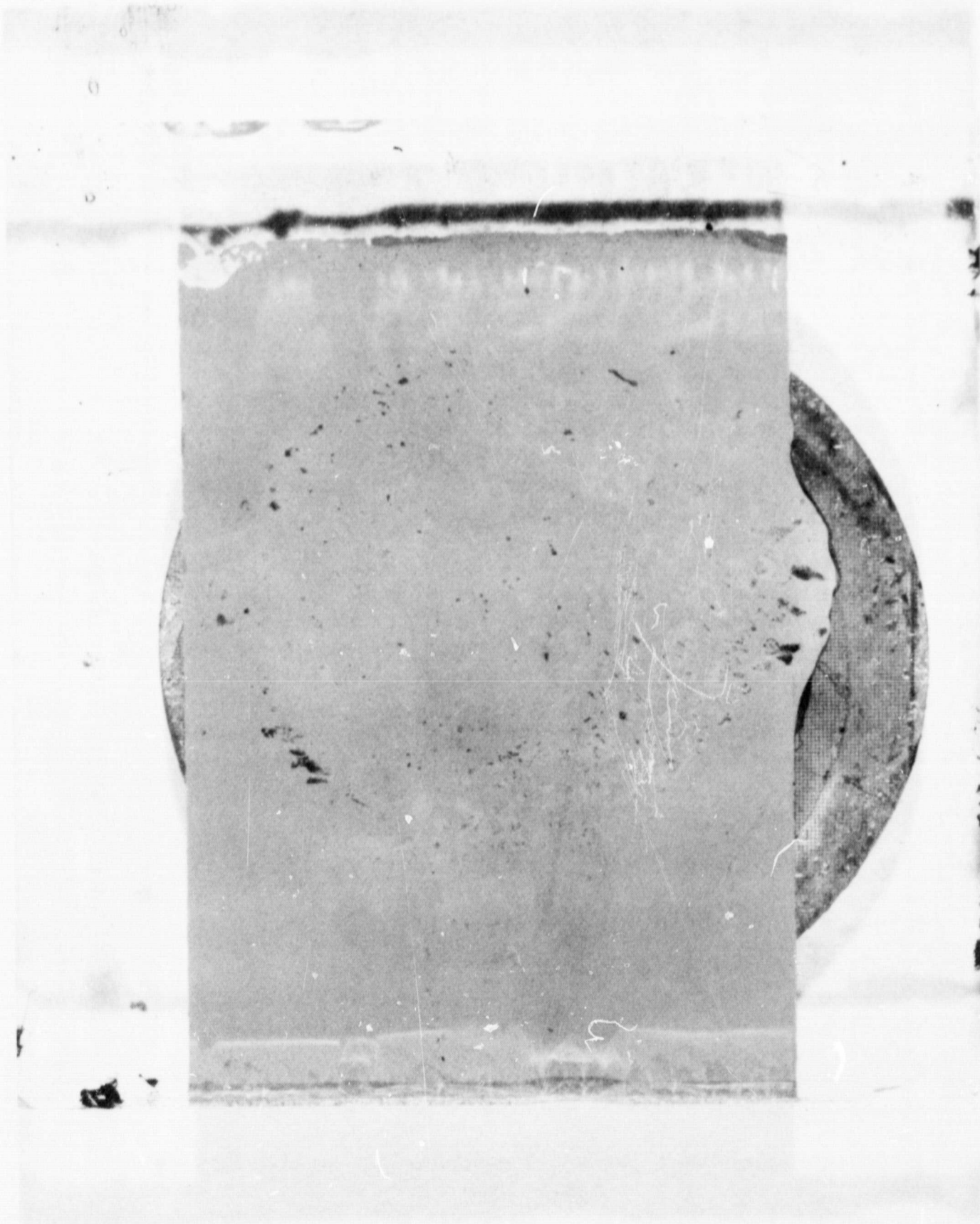
Figure 11

100 x 100 IMAGE PLATE

film of cadmium sulfide photoconductor was then deposited on the electroded ferroelectric and activated. Finally, a gold bar pattern was deposited on the surface of the cadmium sulfide. (See Figure 12). Since all element electrodes are connected by the pattern, this configuration represents a common top and bottom electrode that sandwich the photoconductor and ferroelectric layer.

This configuration was tested initially by fabricating a single line of six elements. A four mil layer of ceramic lead titanate zirconate was covered with a solid electrode on the bottom and dot electroded with gold on the top surface. A thin film photoconductor was then deposited on the combination. Instead of a common bar electrode, a line of dot electrodes was used to permit testing of the individual elements. By probing the electrode dots and introducing light across the pertinent photoconductor gap, the hysteresis loop could be observed to grossly estimate squareness ratio and losses. The amount of charge stored and subsequently read was determined by the application of light pulses. After testing, a common top electrode was deposited to connect all of the elements. With voltage applied, a spot of light was used to sequentially illuminate each element in the line. With an opposite polarity voltage, the cycle was repeated and the charge read out of each element. The oscilloscope traces for both readin and readout are shown in Figure 13. The lower amplitude traces indicate that several cycles were required to fully accomplish storage and discharge. Storage times of one hour were possible with less than 10% degradation.

The moving light spot was provided by a tungsten light source with a 1000 foot lambert output in conjunction with a chopper wheel. A set of six neutral filters provided various levels of illumination. The chopper wheel, with a small slit in its outer periphery, rotated at a speed of approximately two cycles per second. An optical bench with adjustable lenses was used to focus light on the individual elements. A two-axis micropositioner was used to provide final alignment while measuring the various output signals on an oscilloscope.

Upon the basis of these experiments, the hybrid configuration was again used to construct a larger image plate consisting of ten lines of fourteen elements. A one-mil ferroelectric was used as a substrate for a three-micron photoconductive layer. This plate is shown in Figure 14. The photoconductor electrode gaps were 10 mils wide and the ferroelectric elements were 10 mils by 10 mils in area. For initial testing, the common electrode used to connect the ten-line electrodes was deleted. The entire plate was flooded with illumination and voltage was applied sequentially to each line while the composite hysteresis loop was observed for uniformity. From line to line, the loops did not vary by more than 10%. The common electrode was added and a light spot was used to interrogate a line at a time. Initial testing indicated a very low signal to noise ratio that made it impossible to adequately test for gray scale and other performance characteristics.

BAR PATTERN ELECTRODE
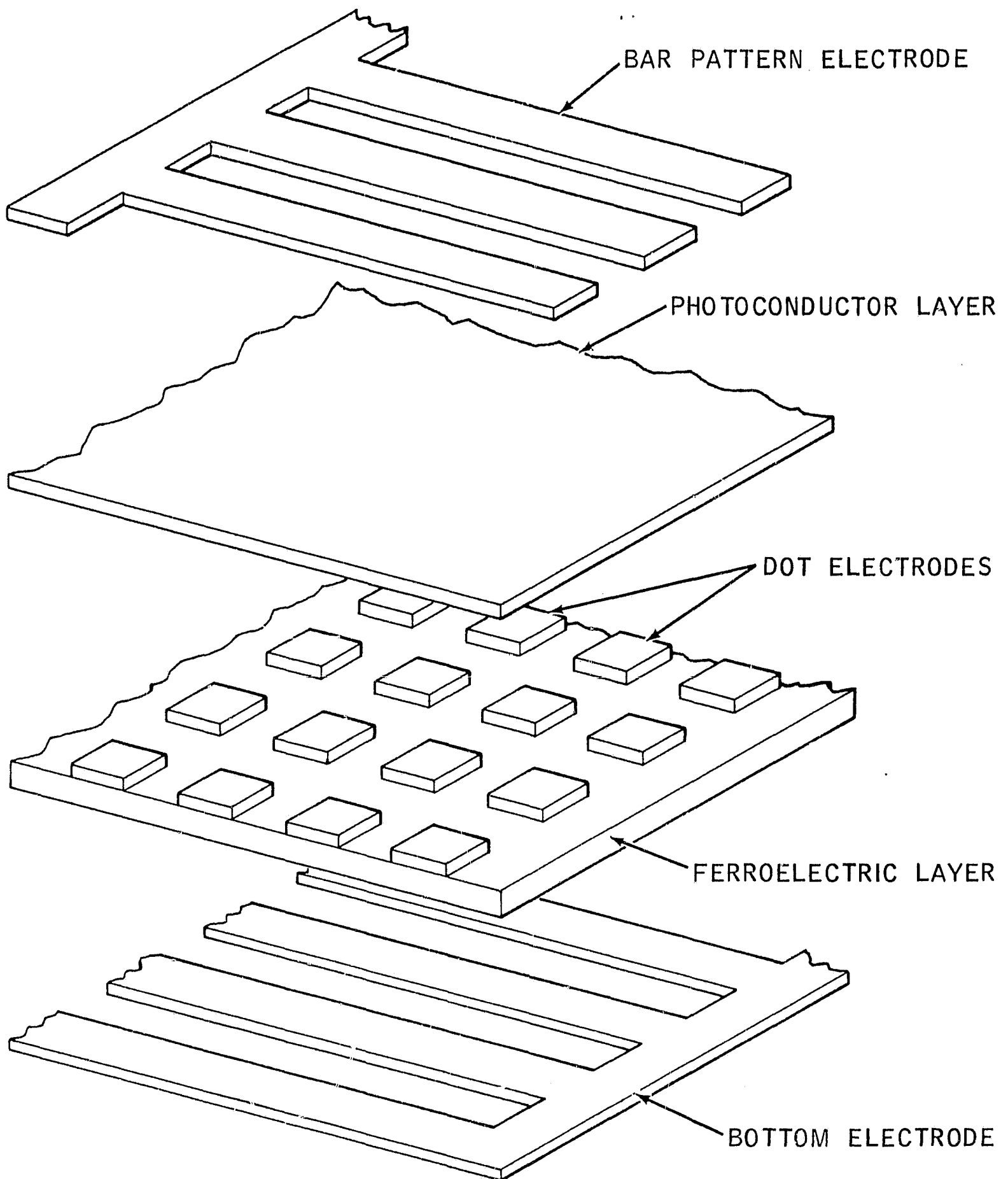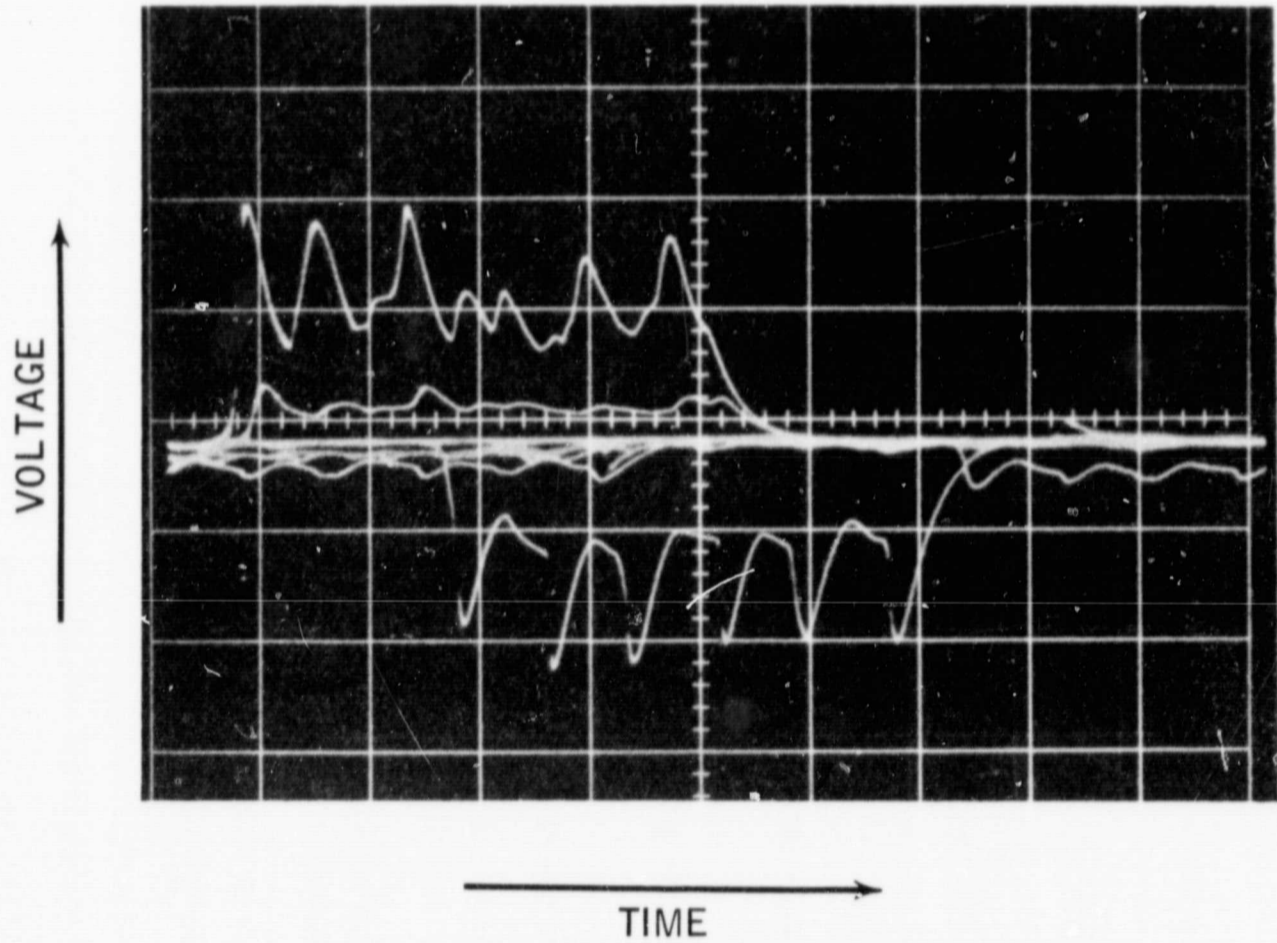
PHOTOCONDUCTOR LAYER

DOT ELECTRODES

FERROELECTRIC LAYER

BOTTOM ELECTRODE

Figure 12

10 x 10 IMAGE PLATE CONSTRUCTION

TIME

HORIZONTAL: 0.2 sec DIV.$^{-1}$
VERTICAL: 1 volt DIV.$^{-1}$
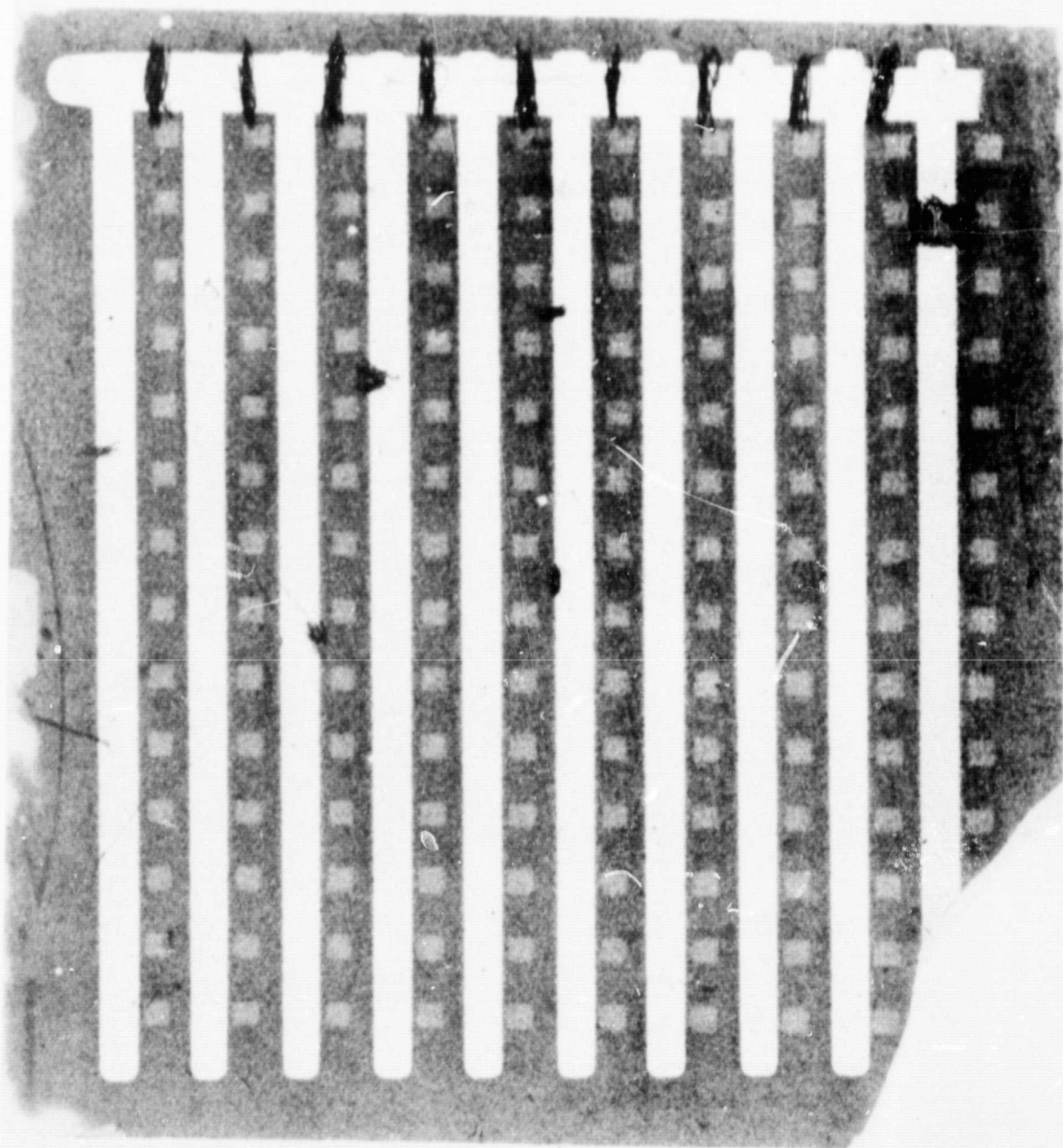
Figure 13

LINE READOUT

Figure 14

10 x 10 IMAGE PLATE

THIN FILM MATERIAL DEVELOPMENT

The fabrication of the Ferrotron image plate in large areas required the development of new thin film process techniques for the preparation of the photoconductor, transparent conductor, and ferroelectric materials. To date, with the exception of the ferroelectric, these developments are essentially completed inasmuch as the established techniques yielded materials better than satisfactory for this application.

Photoconductor

Since a meteorological image sensor demands high uniformity in the electrical as well as optical properties of photoconductors, it is necessary to produce a film which is free of mechanical defects such as pinholes. For example, to use a photoconductor in the volume mode requires a continuous or line and dot electrode pattern on both surfaces of the photoconductor and pinholes will cause electrical shorts. The problem is not as severe for a photoconductor operated in the surface mode but the uniformity is degraded.

A program was initiated to determine the origin and eliminate such defects during the various phases of deposition and post activation.

The 4.0 micron thick CdS film is normally deposited onto glass substrates by evaporating CdS in pellet form from two diagonally spaced sources. The evaporation temperature is kept constant at 700-800oC and the substrates are heated to a very low temperature. After the deposition of CdS, a layer of acceptor and a layer of $CdCl_2$ are deposited over the photoconductor. Each sample is post heat treated to transform the amorphous film into a polycrystalline film.

By illumination of the film from the bottom and side a large number of bubbles became visible over the entire surface area with a high power microscope under 43X magnification. The average diameter of these bubbles was approximately 60 microns. (Figure 15)

Such defects are highly probable due to the hygroscopic nature of cadmium chloride. It was determined from experiment that the formation of the bubbles depends strongly upon when the $CdCl_2$ is introduced into the process.
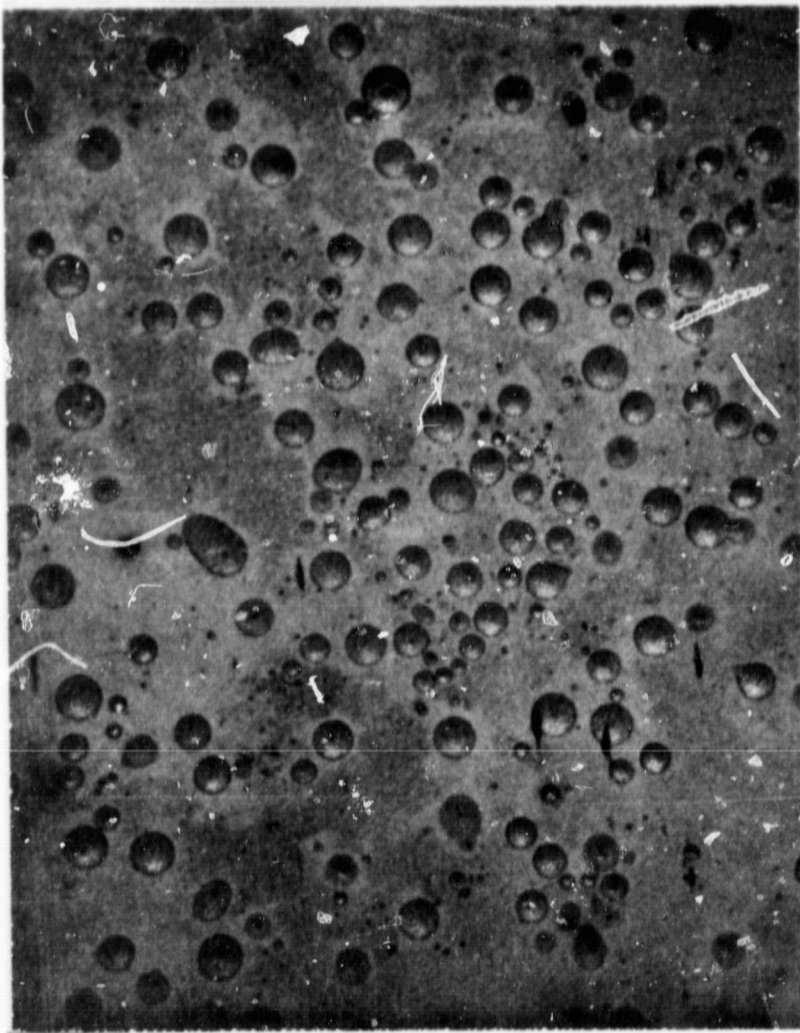
DEPOSITION SEQUENCE: $CdS + Cu + Cd\ Cl_2$
MAGNIFICATION 43X

DEPOSITION SEQUENCE: $CdS + Cu + Cd\ Cl_2$
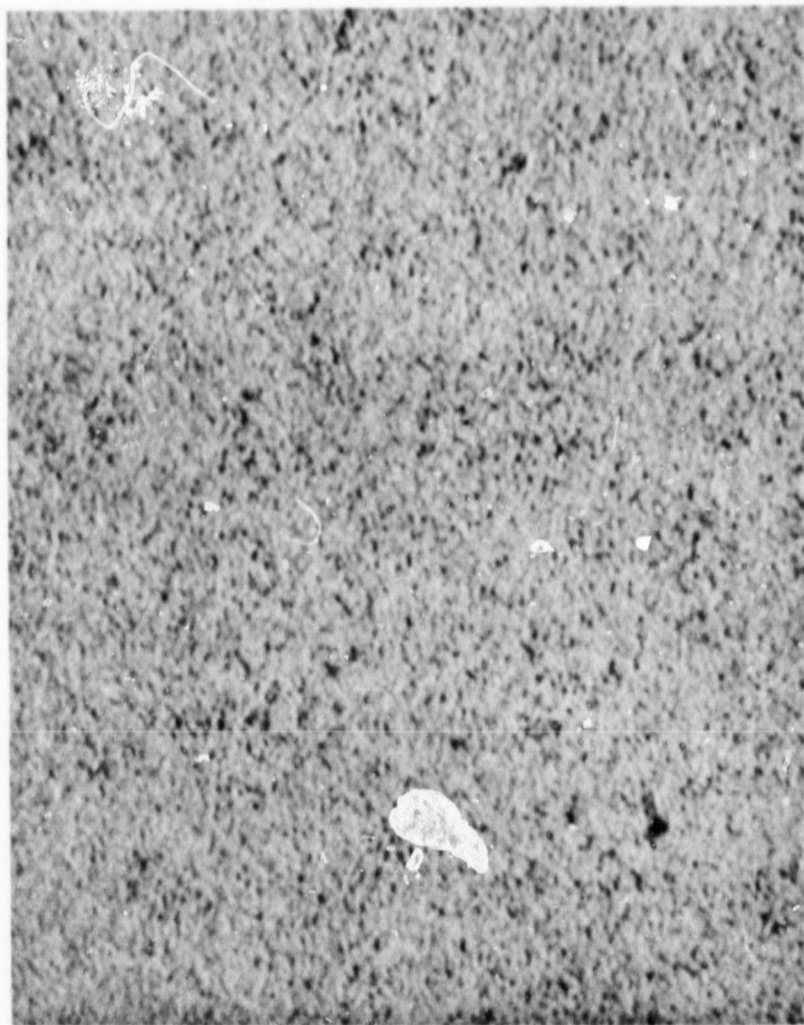MAGNIFICATION 430 X

Figure 15

PHOTOMICROGRAPH OF SURFACE OF DEPOSITED CdS FILM

Four experimental vacuum runs were made for the examination. In the first run the order of deposition of the acceptor material and the flux was changed. The size and number of the bubbles decreased in the run where the CdCl2 was deposited initially. The acceptor was deleted in a second run but the results were ambiguous. During the third run, the flux was deleted and the bubbles did not occur. It, therefore, was concluded that the defect formation could be attributed to hygroscopic cadmium chloride and deposition of the flux prior to the acceptor could minimize the pinhole occurrence. Further tests have proven that slower heat treatment can aid in producing more uniform films. (Figure 16)

Ferroelectric

An entirely new ferroelectric structure was evolved where the Curie temperature is high enough for photoconductor deposition and which can be vacuum deposited onto a substrate, thereby eliminating the fragility problem. This structure is based on a rare earth erbium trioxide material with a bismuth oxide flux and manganese oxide which proves to be chemically stable and shows no fatigue with repeated operation. Figure 17 shows the material's hysteresis loop characteristic which is as good as that obtained with the triglycine sulfide crystal. The Curie point was found to be $500^{\circ}C$ which is commensurate with the photoconductor postactivation temperature. Also, the spontaneous polarization and the coercive field (though high) were acceptable.

The development of this rare earth ferroelectric compound in thin film form under Marquardt Research and Development and contracted efforts has evolved from an original investigation of barium titanate. This latter material has marked limitations in material properties for the present application being considered over these newer compounds. For example, barium titanate, due to its domain structure, exhibits fatigue, crystalline strain under applied voltage and incompatibility in coefficient of expansion with cadmium sulfide. The rare earth compounds, on the other hand, although reported only to a limited extent in the literature, have single type domains, high Curie temperature, low polarizability and very short switching times, important properties in the operation of the solid state sensor. In addition, the chemical stability, inherent in most oxides, would assist in the interface between the ferroelectric and photoconductor materials.
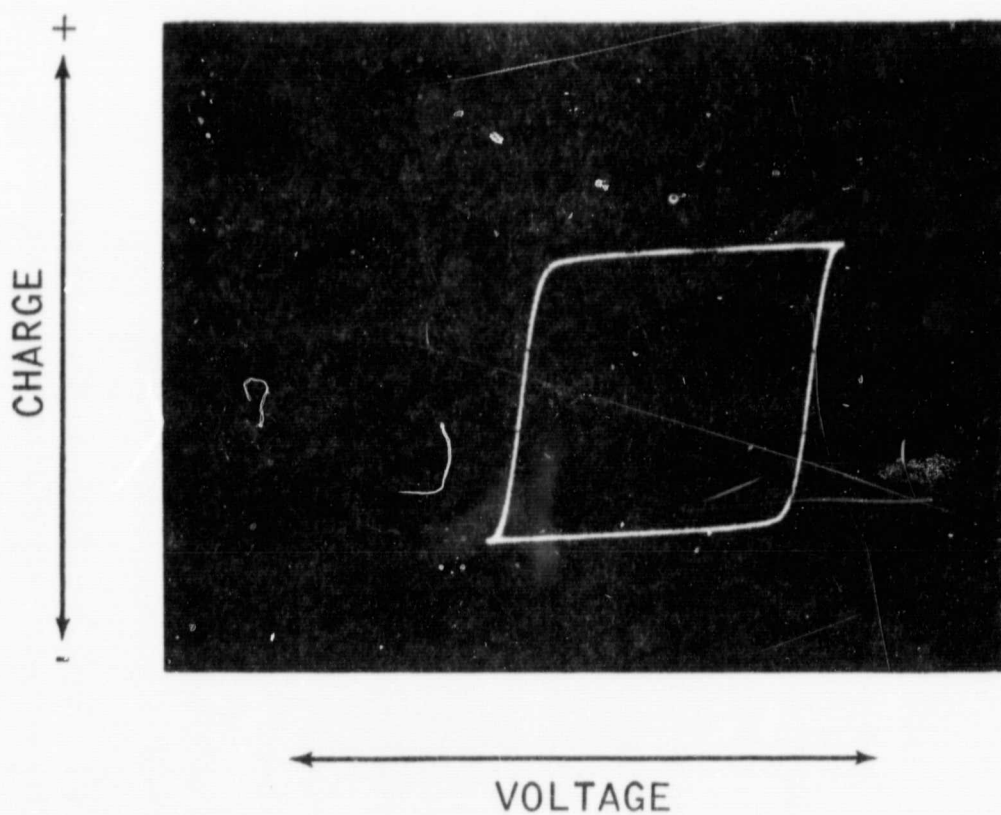
DEPOSITION SEQUENCE: $CdS + Cu + Cd\ Cl_2$
MAGNIFICATION 940 X
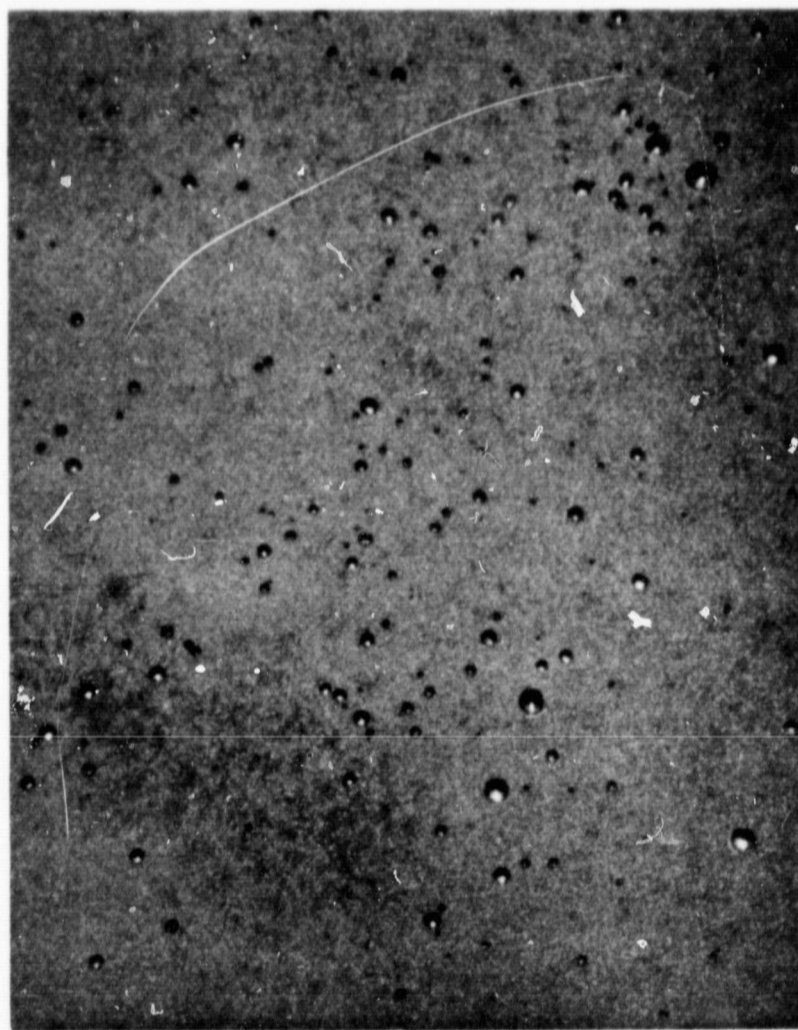
DEPOSITION SEQUENCE: $CdS + Cd\ Cl_2 + Cu$
MAGNIFICATION 43X

Figure 16

PHOTOMICROGRAPH OF SURFACE OF DEPOSITED CdS FILM

CHARGE

VOLTAGE

HORIZONTAL: 2 VOLTS PER DIVISION
VERTICAL: 10^{-9} COULOMBS PER DIVISION

Figure 17

HYSTERESIS LOOP OF RARE EARTH TRIOXIDE FERROELECTRIC
(DEPOSITED FILM)

The performance characteristics of this new ferroelectric material closely resemble those of triglycine sulfate (TGS) with the exception of Curie temperature (temperature at which the material loses its ferroelectric properties) which is at least ten times greater than that for TGS, coercive voltage which is about twice that for TGS and the above mentioned conductivity. The higher Curie temperature is important in the operation of a sensor plate in higher than normal environmental conditions and at the same time may provide a considerably simplified fabrication technique. The higher coercive voltage, although not an advantage in itself, only represents a slight increase in operating voltage; for example, a 10 micron thin film of the ferroelectric material requires an operating voltage of from 3 to 4 volts.

Marquardt's present investigation of these compounds has been based on both Erbium and Yttrium rare earth oxide mixed in stoichiometric ratios.

The same experimental procedure has been applied with both Erbium and Yttrium rare earth oxide mixed in stoichiometric proportions with either manganese sesqui or dioxide. A solvent was introduced in a 10/1 molar ratio, either as bismuth trioxide or lead fluoride, the latter forming larger single crystals of the compound than the former. With either solvent, platinum containers were unsatisfactory; since M_nO is strongly reducing at the processing temperature, a platinum eutectic was formed with either lead or bismuth that evaporated during the firing cycle. Pure alumina was not attacked by PbF_2, but is less satisfactory with Bi_2O which dissolves it very slightly. The most satisfactory crucibles were made of dense Zirconium oxide though the fired mixture wets very well the crucible and is somewhat more difficult to retrieve.

Since all manganese oxides reach the same composition above 950^oC, i.e., $MnO + Mn_3O_4$ with a vapor pressure of approximately a tenth of an atmosphere, all compounds prepared on a stoichiometric basis did show, in chemical analysis, a loss of manganese.

All materials were used with 1 ppm purity, yet contaminations attributed to crucible and furnace lining were found during analyses. See Table

All melts were prepared under the same temperature cycling with a plateau at 1300° whose duration determines the residual content in Bismuth or lead. It has been observed that in order to maintain less than one percent in bismuth the baking time exceeded 60 hours. The least fluoride flux for the same proportion didn't require more than 25 to 30 hours.

For melts used in vacuum evaporation, quick cooling was found to be satisfactory whereas for the growth of platelets for x-ray, analyses required cooling rate smaller than 15° per hour to produce crystals that didn't exceed 2 mm in length.

34

In processing the material at high temperature, in a high or low pressure of oxygen, Mn will assume a valence state from Mn^{4+} to Mn^{2+}, with the desired valence Mn^{3+} somewhere in between. Hence, even with a coordination number of six, relatively high conductivity would occur when one type of atom presents itself in two different states of valency at the same time. Use has been made of this property to confer definite semiconducting properties of the compound which are reported below.

The state of valency is not detectable in x-rays and the procedure was corrected on a trial basis, by introduction of well dried nitrogen with a volume flow percentage of carbon dioxide between 2 to 5 percent.

Evaluation of the vacancies produced by the introduction of Mn^{3+} - Mn^{2+}, has been attempted, but is not completed to date and work continues in that area in order to categorize fully the resulting P type semiconductor. The melts obtained from the above procedure were ground and sieved to obtain small particles between 10 to 40 microns and stored in plastic containers.

Films were produced either by refiring electrophoretically deposited powder, without flux addition, on a strip of platinum for rapid testing of the melt properties, or by flash evaporation technique in vacuum.

The remelted films were homogenous down to one mil thickness. Good ferroelectric properties were obtained when the refiring time was short and was stopped just as the powder wetted the platinum surface. Resistivity of these films was between 10^7 to 10^8 ohm-centimeters. Longer firing times produced lower resistivity. Squareness ratios greater than 80 were obtained at 60 cycles and good hysteresis loops were measured up to one megacycle frequency. The coercive voltage for these films was 2,000 volts cm^{-1}, approximately three times greater than barium titanate at the same frequency. Polarizability was very consistent over large areas with the measurements fluctuating between 2.5 and 3 microcoulombs-cm^{-2}. Films produced by refiring the melt powder have been operated over several months without any observable variation in characteristics.

The flash evaporated films were produced using an iridium strip heated by electron bombardment. The finely ground and sieved powder is dropped on the heated substrate at a constant rate so as to maintain a partial vapor pressure of 10^{-5} Torrs. Films deposited at low substrate temperatures below 700°C have poor ferroelectric properties. At substrate temperatures above 850°C, a definite organization is obtained in these films, although the structure is polycrystalline. Magnesium oxide cleaved crystal substrates did not produce any epitaxial growth. Aluminum oxide single crystals were the most satisfactory substrates for producing semi-epitaxial growth of Erbium-manganese-oxide ($ErMnO_3$) films

at temperatures between 850 and 900°C. At this time, x-ray analysis of these films has not been completed, but the patterns obtained seem to provide a very well organized structure.

The principal problem has been the higher than desirable conductivity of these films. X-ray mass spectrometry (Table I) does not show any differences in stoichiometry between the evaporated thin films and the bulk material. It is assumed that the higher conductivity (10^{-7} mhos-cm^{-1}) is due in part to a change in valency of one of the elements and thereby creation of vacancies when the film is processed on reactive substrates.

Further development of the thin film ferroelectric material will require the completion of an electro-chemical analysis which will permit modifications in the rare earth trioxide constituents to overcome the presently higher than desirable bulk conductivity. The basic deposition process for this rare earth ferroelectric has been well defined by previous experimentation under other contracts and is based on flash evaporation techniques in which the material is slowly fed in powder form to a preheated evaporation boat. Although considerable progress has been made to reduce the conductivity value, the effort required to achieve the necessary improvement was considered outside the scope of the present program.

A lead titanate zirconate ceramic compound was investigated as an alternate ferroelectric material which appeared to overcome all the above difficulties. Originally, it was felt that such a material could not be produced in the required thickness. The development of a vacuum deposition process was found to be a difficult technological problem because of the fact that the various constituents of the compound have very different melting points and vapor pressures resulting in a non-stoichiometric material layer. Excluded from further investigation was another vacuum approach where the constituents are deposited individually because the overall process proved too time consuming.

Good results were obtained with ceramic stock material prepared by hotpress techniques. Lead titanate zirconate raw material was prepared with a special ratio of its constituents for best performance characteristics in this application. Slates of 2 mil thickness were prepared from the raw material by a grinding process. They proved to be quite rugged and could easily be handled during the electroding process. Figure 18 shows the hysteresis loop pattern across a larger area slate indicating a relatively good uniformity which is desirable in the Ferrotron image plate. The Curie temperature is about 250°C allowing the photoconductor to be deposited directly onto the slate. The squareness ratio is not quite as good as that obtained with the rare earth material but appears to be acceptable. No difficulties were experienced in regard

TABLE I

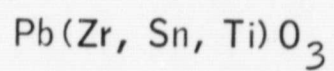Spectrographic Analyses

Impurities Detected in Percent

Compounds	Mn	Y	Er	Bi	Pb	Al	Mg	Fe	Si	Cr	Ni	Cu	Ca
Y Mn O$_3$	10	65	5	1	0	1	0.01	0.1	0.3	0	0	0.1	0.01
Y Mn O$_3$	28	60	0	0	1.5	0.1	0.01	0.1	0.1	0	0	0.01	0.01
Er Mn O$_3$	15	0.05	30	3	0	0.5	0.01	0.1	0.1	0	0	0.01	0.01
Er Mn O$_3$	35	0.01	45	0	0.5	0.1	0.01	0.1	0.1	0	0	0.01	0.01

ACTUAL SIZE

50 X
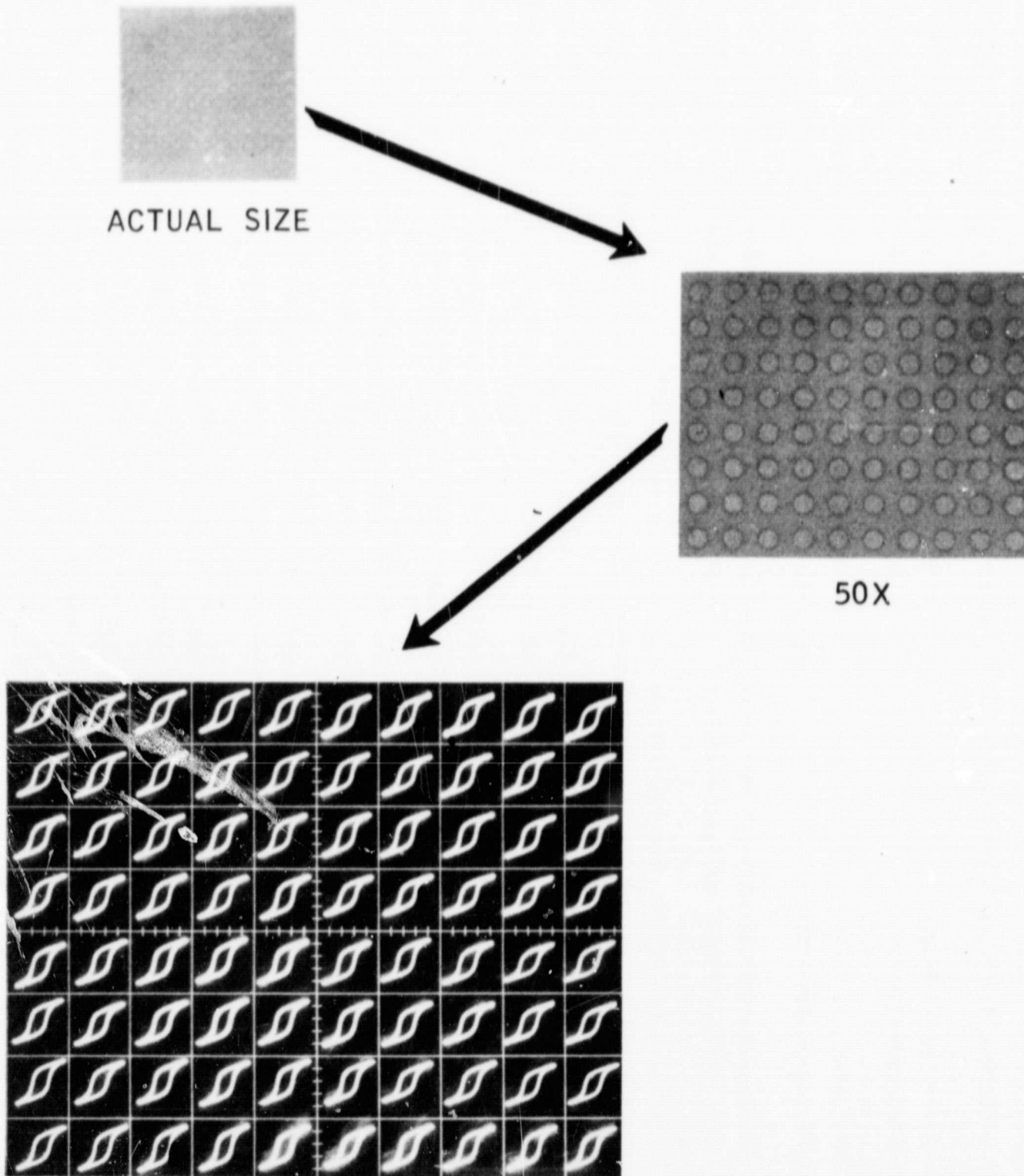
HYSTERESIS LOOP PATTERN

Figure 18

ELECTRODED FERROELECTRIC CERAMIC SAMPLE

$Pb(Zr, Sn, Ti)O_3$

to conductivity. Figure 19 shows the result of an experiment with a
single Ferrotron cell employing this material. The open loop indicates
the charge accumulated when the photoconductor receives full light and
straight line represents the condition for the photoconductor in the
dark. Although an excellent control was obtained, the photoconductor
had to be operated in the surface mode because the coercive voltage
required to operate a 2 mil thickness of the material was too high for
operation with a volume photoconductor.

Realizing that the above process is impractical for producing,
economically, the lead titanate zirconate material in larger area with
the desired thinness, the development of an entirely new deposition
process was initiated. Recently, a significant state-of-the-art advance-
ment has been accomplished inasmuch as uniform layers of 2 x 2 inches
were produced with a thickness of only a fraction of a mil. The material
itself features the same advantageous properties as reported above for
the ceramic slate. Furthermore, because of its thinness it can be oper-
ated with the desired small coercive voltage. Figure 20 shows the
hysteresis loop characteristic indicating the low voltage operation and
a good squareness ratio.

The new deposition process is based on a liquid/spinning technique
which ultimately could produce layers as thin as a few microns due to
the liquid solution which is composed of atomic size particles rather
than grain size particles as in the above hot press process. Further-
more, another significant objective has been accomplished by establishing
a process where the ferroelectric material is formed only in small ele-
mental areas which is desirable in an image plate because it reduces the
crosstalk between adjacent elements. The formation of elements is pro-
duced by activating the deposited material only in the desired areas
and the remainder of the material behaves as a linear material of low
dielectric constant.

Figure 21 illustrates, in detail, the procedure which has been
developed for the preparation of the lead titanate zirconate layer.
As a first step, a platinum electrode is deposited on an alumina sub-
substrate. This combination is then coated with a solution consisting
of the halides suspended in alcohol. A subsequent spinning operation
evaporates the alcohol. The material is then fused at an elevated
temperature of approximately $1000^{\circ}C$. The next step consists of the
deposition of lead in small elemental areas through a conventional
mask. The lead is then diffused into the material at a temperature of
$500^{\circ}C$. An activator flux is deposited over the whole surface and a
temperature of $1300^{\circ}C$ is used for activation. The result is a thin film
consisting of polycrystalline ferroelectric areas isolated by a low
conductivity, low permittivity dielectric material. A conventional
electrode deposition of gold completes the process. (Figure 22 and Figure 23)

CHARGE

VOLTAGE
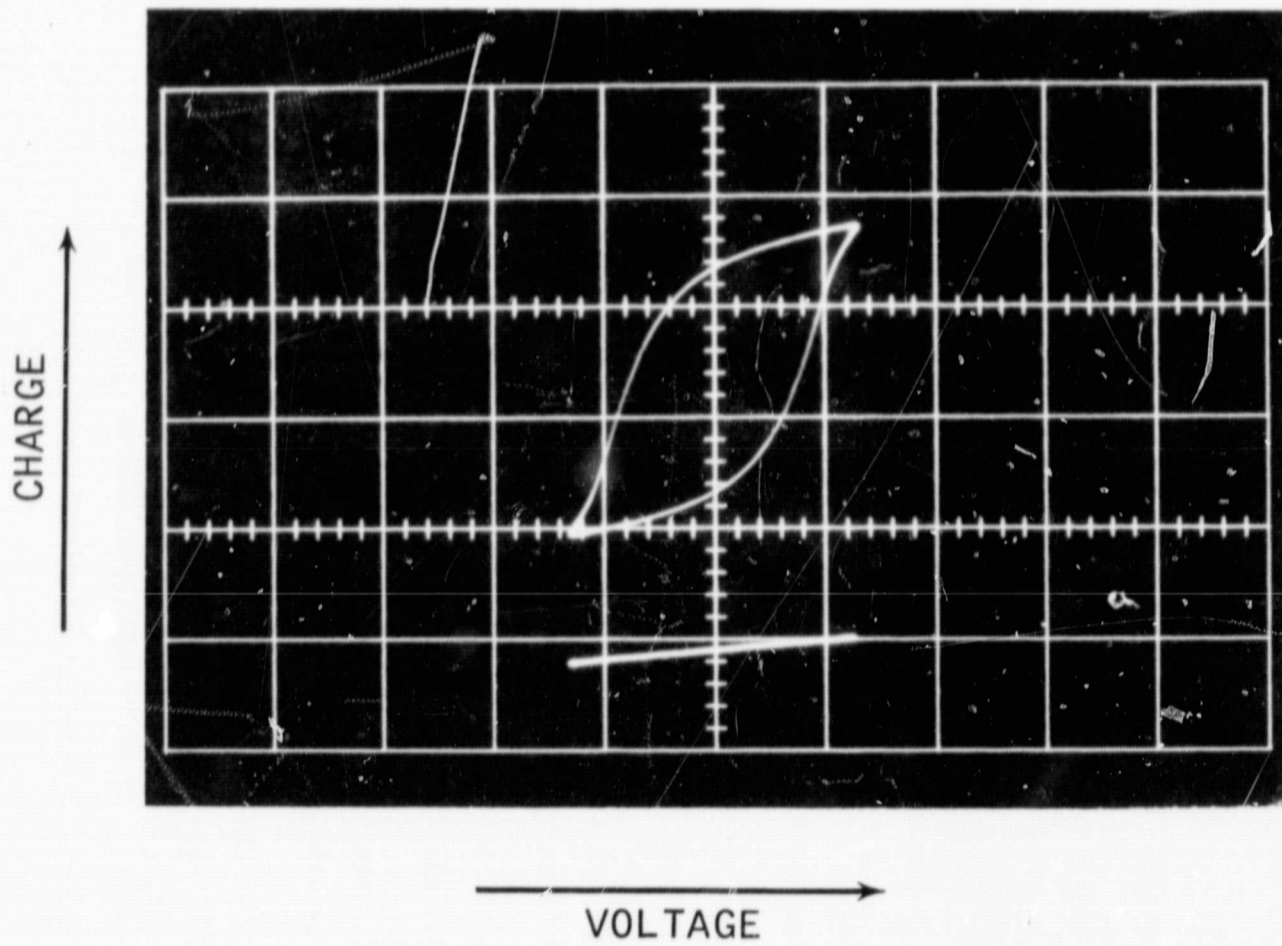
HORIZONTAL: 20 volts DIV.$^{-1}$

VERTICAL: 2×10^{-9} coulombs DIV.$^{-1}$

Figure 19

HYSTERESIS LOOP OF PZT FERROTRON CELL

CHARGE

VOLTAGE
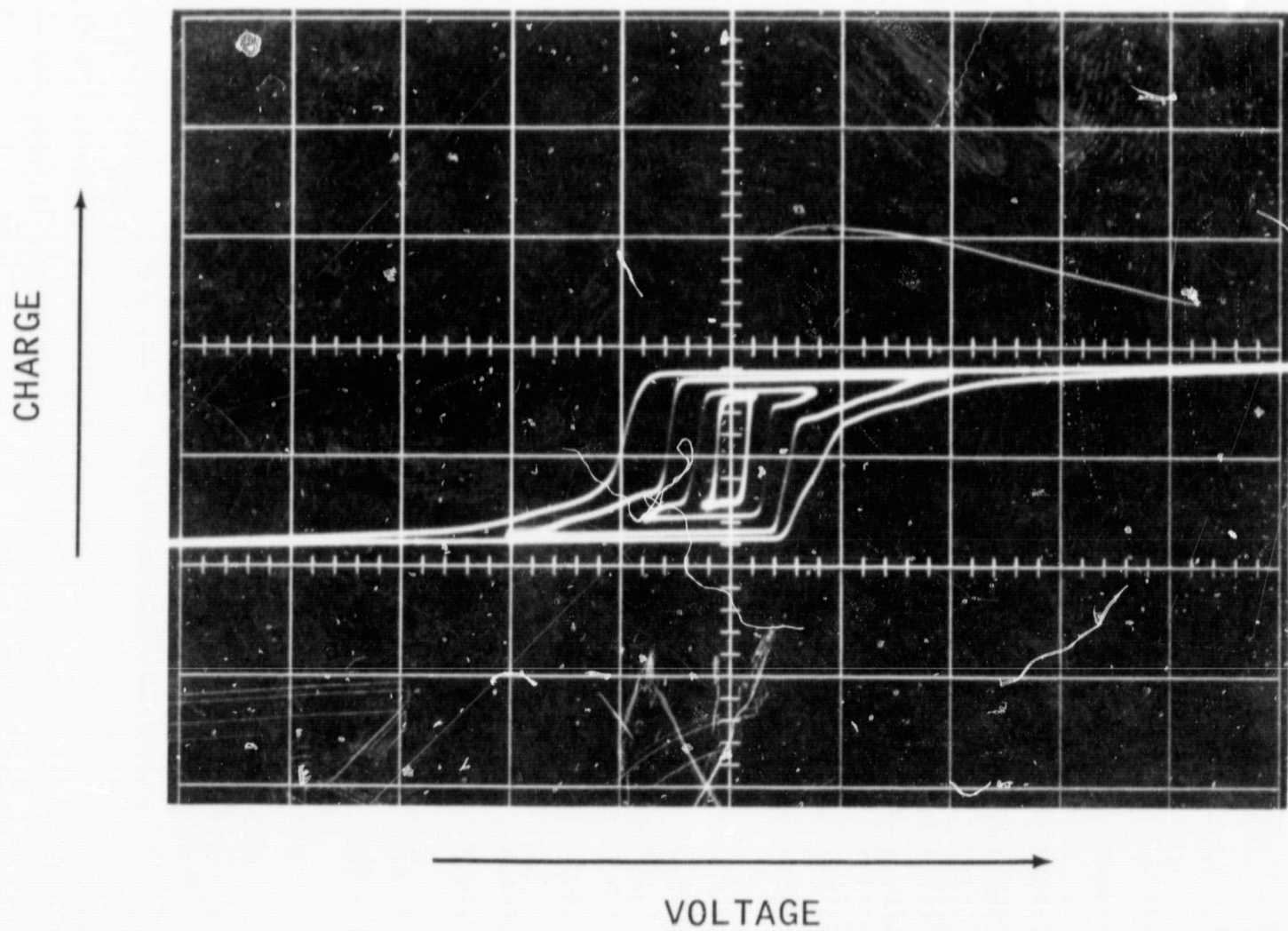
HORIZONTAL: 2 VOLTS PER DIVISION
VERTICAL: 5×10^{-9} COULOMBS PER DIVISION
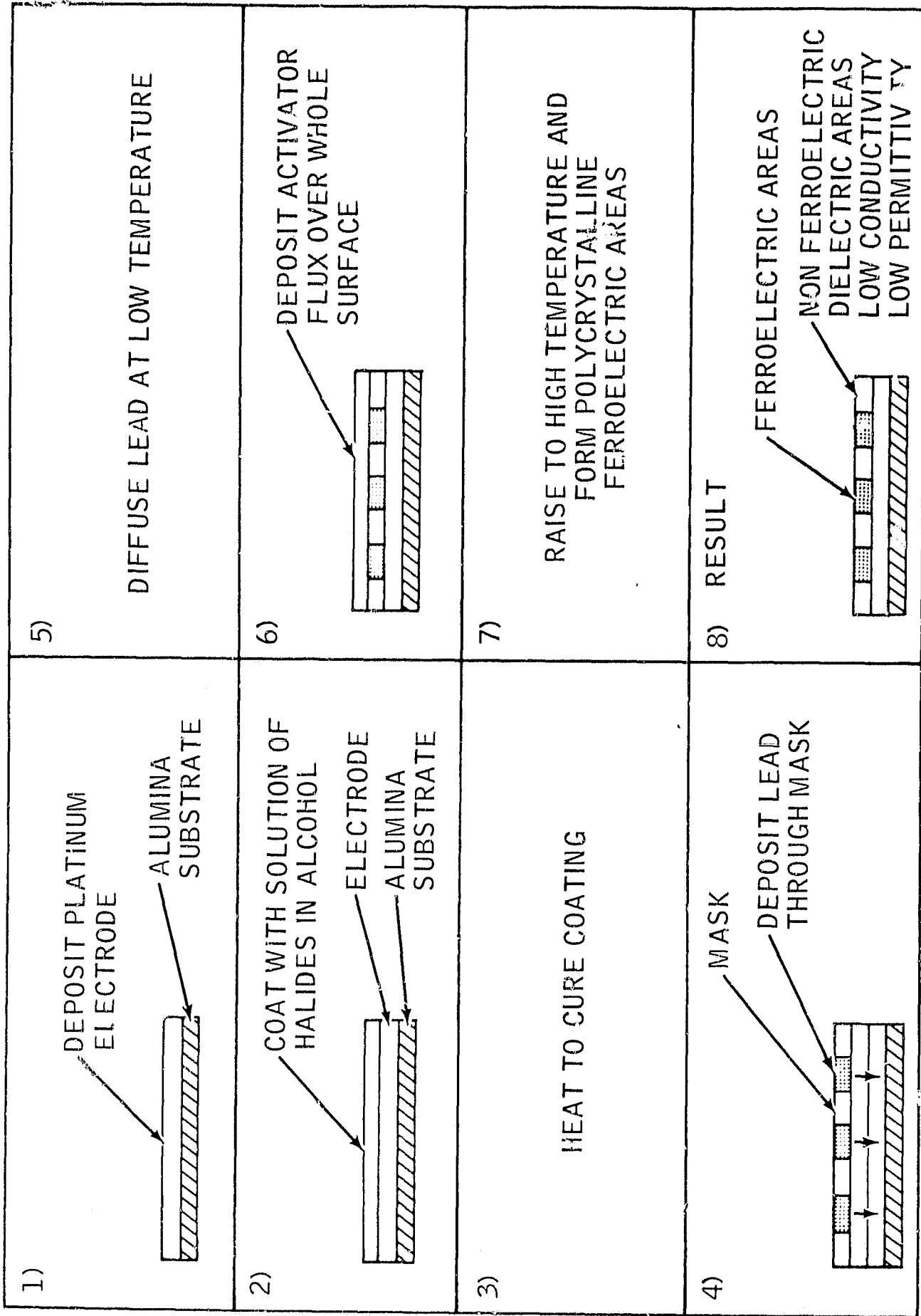
Figure 20

HYSTERESIS LOOP OF PZT FERROELECTRIC

Figure 21

FERROELECTRIC PROCESS
(LEAD-ZIRCONATE TITANATE)

5) DIFFUSE LEAD AT LOW TEMPERATURE

6) DEPOSIT ACTIVATOR FLUX OVER WHOLE SURFACE

7) RAISE TO HIGH TEMPERATURE AND FORM POLYCRYSTALLINE FERROELECTRIC AREAS

8) RESULT

FERROELECTRIC AREAS

NON FERROELECTRIC DIELECTRIC AREAS LOW CONDUCTIVITY LOW PERMITTIVITY

1) DEPOSIT PLATINUM ELECTRODE

ALUMINA SUBSTRATE

2) COAT WITH SOLUTION OF HALIDES IN ALCOHOL

ELECTRODE
ALUMINA SUBSTRATE

3) HEAT TO CURE COATING

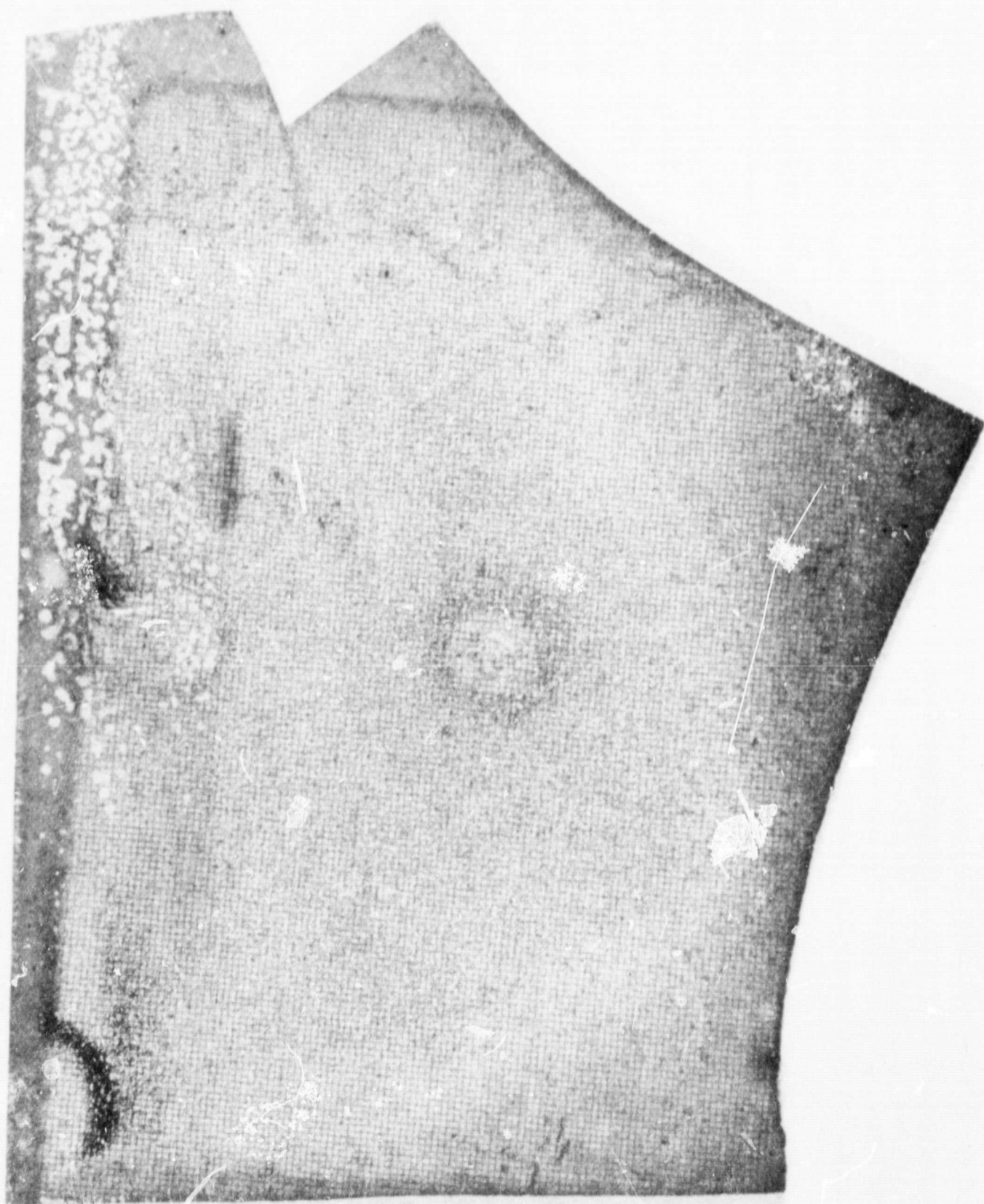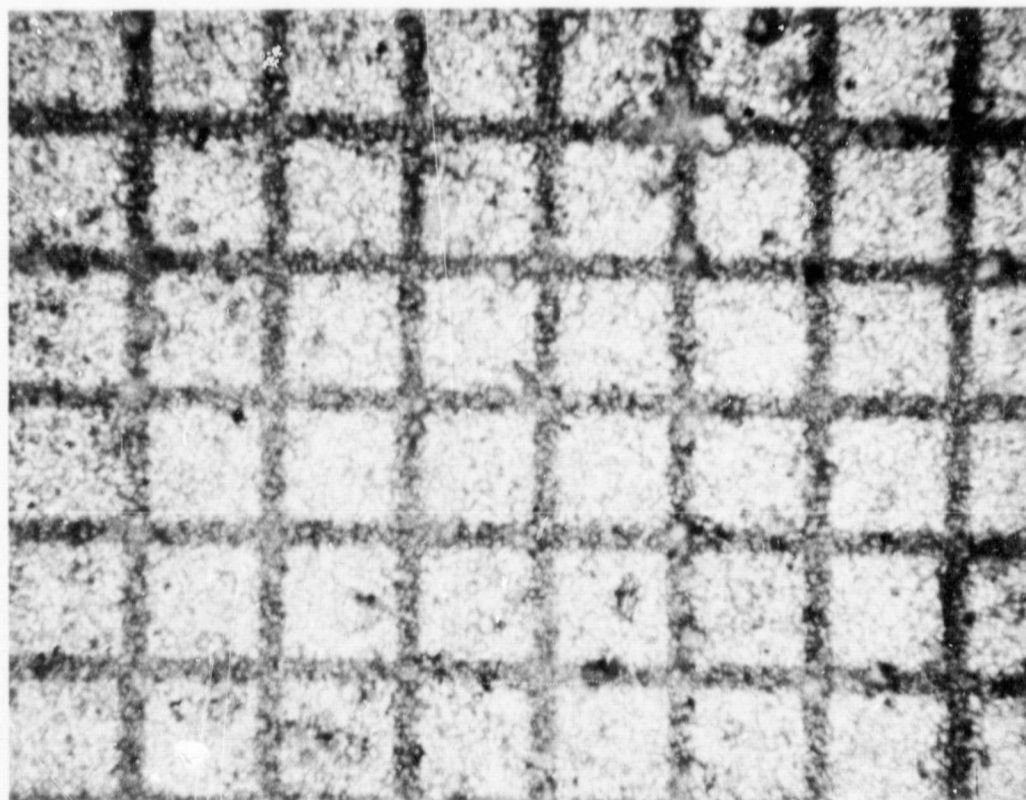4) MASK

DEPOSIT LEAD THROUGH MASK

Figure 22

THIN FILM FERROELECTRIC

150 X

Figure 23
THIN FILM FERROELECTRIC MICROGRAPH

Although the development of the basic ferroelectric material process was successful and is essentially completed, the equipment for producing a ferroelectric layer in image plate format requires a considerable refinement. In particular, the post activation device has to be redesigned completely. The difficulties in developing such an equipment stems from the fact that: (1) the deposited ferroelectric layer has to be heated to a very high temperature of about 1300°C without contamination by the heater material, (2) the lead vapor tends to dissolve any receptacles required for holding the ferroelectric substrate, and (3) the heat has to be applied very uniformly within an accuracy of a few percent to prevent warping of the substrate. The latter factor is the primary reason for failing to make a complete image plate with this material.

As a result of the above development, the photoconductor and ferroelectric processes are adequate to produce the sensing and storage materials that can fulfill the requirements of an image sensing plate. However, refinement of the ferroelectric process is necessary for the production of large area plates.

CONCLUSIONS AND RECOMMENDATIONS

Based on the work performed to date in investigating image sensing techniques and the results obtained the following conclusions were reached:

The Ferrotron image sensor is a practical device for providing the large operating range and long term image storage required in a meteorological image transducer as indicated by tests on a line array.

The stored image can be read out optically by a sweeping light beam to suit a specific application.

The image sensor can be fabricated by successively depositing thin films of photoconductor, ferroelectric and electrode materials. The deposited material layers are chemically, physically and electrically compatible and show no deterioration with age or repeated operation as indicated by periodical testing over a period of two months.

The development of the low voltage, thin film, ferroelectric material is needed to allow the preparation of higher resolution and larger area image plates.